Copy
RM L52I09

6

NACA

RESEARCH MEMORANDUM

ANALYTICAL STUDY OF STATIC AND LOW-SPEED PERFORMANCE OF THIN PROPELLERS USING TWO-SPEED GEAR RATIOS TO OBTAIN OPTIMUM ROTATIONAL SPEEDS

By Jean Gilman, Jr.

Langley Aeronautical Laboratory
Langley Field, Va.

NATIONAL ADVISORY COMMITTEE
FOR AERONAUTICS

WASHINGTON

November 5, 1952

NATIONAL ADVISORY COMMITTEE FOR AERONAUTICS

RESEARCH MEMORANDUM

ANALYTICAL STUDY OF STATIC AND LOW-SPEED PERFORMANCE OF THIN PROPELLERS USING TWO-SPEED GEAR RATIOS TO OBTAIN OPTIMUM ROTATIONAL SPEEDS

By Jean Gilman, Jr.

SUMMARY

A study has been made to determine the effect of variable propeller gearing on the low-speed performance of modern thin-blade propellers. Inasmuch as experimental propeller data over a suitable range of operating conditions are currently lacking, and because of the scarcity of suitable airfoil data, it was necessary to devise methods of estimating the performance. The methods used are based on optimum loading considerations.

Results from the analysis of a sample flight problem indicated that, for propellers having a design advance ratio of 2.0, peak values of static thrust and take-off thrust occur at approximately the same rotational speed used for high speed. If the design advance ratio is 3.0 or higher, variable propeller gearing should be used for low forward speeds because the rotational speed corresponding to high speed is too low and hence the propellers are overloaded at low speeds. By incorporating variable gearing to increase the rotational speed, the propeller loading is reduced with a consequent gain in thrust. This gain in low-speed thrust due to reducing the propeller loading increases as the design advance ratio is increased; for a design advance ratio of 4.0, the gain in take-off thrust amounts to 30 percent or more. When a given power is absorbed at optimum rotational speeds, the static and take-off thrusts of propellers having high design advance ratios are higher than the static and take-off thrusts of propellers having lower design advance ratios. For a given power requirement this optimum rotational speed becomes lower as the design advance ratio is increased.

For rotational tip Mach numbers up to about 1.2, calculations show that thin propellers incorporating moderately cambered airfoil sections produce peak static thrusts which are 15 to 20 percent higher than the peak static thrust with symmetrical sections. When a rotational tip Mach number of about 1.2 is exceeded, there is a substantial drop in peak static thrust.

INTRODUCTION

In the early history of airplane propellers adequate performance was obtained through the use of fixed-pitch propellers. Then, as engine powers and airplane speeds were increased, the performance of the fixed-pitch propeller became inadequate. This inadequacy was overcome by the development of the constant-speed propeller. The constant-speed propeller gave improved performance for two reasons: One, the constant-speed mechanism allows the engine to operate at rated power as needed and, two, a constant-speed propeller operates at or near peak efficiency over a larger range of flight conditions than does the fixed-pitch propeller. For certain combinations of speed, power, and altitude, a constant-speed propeller which has been selected on the basis of top-speed considerations only will give good performance at other flight conditions including the take-off. There are other combinations of speed, power, and altitude where emphasis on a particular flight condition will unduly penalize the over-all performance; for such cases it has been common practice to select a compromise constant-speed propeller. For still other combinations of speed, power, and altitude it becomes very difficult to make a suitable compromise using constant-speed propellers. In some of these latter cases it is possible to use two-speed gearing to overcome the difficulty.

Current progress in the development of turboengines in conjunction with thin-blade propellers offers attractive performance possibilities at airplane speeds well up into the transonic region. For such applications it is desirable to emphasize the high-speed conditions in the design of the propeller. Such emphasis is likely to result in poor take-off characteristics; hence the applicability of two-speed gearing appears to be of greatest interest in regard to this type of installation. The purpose of the present paper is to investigate the effect of two-speed gearing on the take-off efficiency under certain conditions.

Experimental data on thin-blade propellers are currently unavailable in sufficient quantity for performance analysis at low airspeeds. By treating the induced losses and drag losses separately, however, it is possible to obtain a preliminary estimate of the propeller efficiency through analytical means. The present paper gives charts from which the efficiencies can be readily computed for optimum rotational speeds. Sample calculations for simulated flight conditions are given. Also included is a brief discussion of the static thrust of thin propellers, including the effect of camber on the static thrust.

[redacted]

SYMBOLS

a	speed of sound, ft/sec
B	number of blades
b	blade width (chord), ft
C_P	power coefficient
C_Q	torque coefficient
C_T	thrust coefficient
c_d	section drag coefficient
c_l	section lift coefficient
C_L	airplane lift coefficient
c_{l_d}	design lift coefficient
D	propeller diameter, ft; also drag, lb
G	Goldstein induced-velocity-correction factor for a finite number of blades
h	blade section maximum thickness
J	advance ratio, V/nD
$K(x)$	Theodorsen's circulation function
L	lift, lb
$\overline{L/D}$	nominal L/D of propeller operating at static thrust, related to L/D at the 0.7R station by an empirical factor, $\frac{\bar{L}}{D} \approx \frac{1}{3}\left(\frac{L}{D}\right)_{0.7R}$
M	Mach number of advance, V/a

[redacted]

M_x section resultant Mach number, $M\sqrt{1+\left(\frac{\pi x}{J}\right)^2}$, or, $M_x = xM_R$ when $J = 0$

M_R tip rotational Mach number, $\pi nD/a$

n propeller rotational speed, rps

P power, $\frac{\text{ft-lb}}{\text{sec}}$

P_{C_V} power coefficient, $P/\rho V^3 D^2$

R propeller-tip radius, ft

r radius to blade element, ft

S wing area, sq ft

T thrust, lb

u slipstream velocity of actuator disk (final wake), ft/sec

V velocity of advance, ft/sec

W resultant velocity at blade section, ft/sec; also airplane weight, lb

w rearward displacement velocity of helical vortex surface

$\bar{w}$ velocity ratio, w/V

x fraction of propeller-tip radius, r/R

x_o radius ratio at spinner juncture

α_i induced angle of attack, deg

β blade angle, deg

$\gamma = \tan^{-1}\frac{c_d}{c_l}$

η efficiency, JC_T/C_P or TV/P

η_i induced efficiency

[redacted]

η_o	profile efficiency
ρ	air density, slug/cu ft
ρ_o	air density for NACA sea level
σ	solidity, $Bb/\pi Dx$
ϕ	aerodynamic helix angle, deg
ϕ_o	geometric helix angle, $\tan^{-1}\frac{J}{\pi x}$

Subscripts:

x	at station x
0.7R	at 0.7 radius station
1	initial conditions
2	final conditions
TO	at take-off
i	denotes induced values

ANALYSIS AND BASIC DATA

In broad outline, the method of analysis presented herein follows, with some modifications, the same procedure given in reference 1. By this procedure the induced losses and profile-drag losses are considered separately and the results are combined to obtain the over-all efficiency. The profile-drag losses are dependent on the airfoil characteristics and so a brief discussion of Mach number effects on the characteristics of thin airfoils, with the consequent effect on profile efficiency, is given.

Propeller performance is dependent on engine characteristics and, since it is considered that the turboengine is the most practical engine for application to the high speeds expected in the near future, the pertinent features of the turboengine are considered in a generalized manner.

The steps involved in analyzing a given propeller-performance problem with turboengines (or any engine the operating characteristics of which are known) are then briefly summarized. A short method of estimating the static thrust of thin propellers completes the presentation.

[redacted]

Induced Efficiency

Reference 1 presents propeller selection charts in which the basic propeller parameters are interrelated in such a manner as to facilitate the selection of a propeller for a given design condition. In reference 2 the results are extended to include propeller operation at values of J less than 1. The results in references 1 and 2 also provide a short method of propeller-performance analysis which saves a considerable amount of time with only a small loss in accuracy over more complete strip-theory procedures.

The present analysis is concerned with propeller-performance problems including variable rather than fixed gear ratios. For such problems it is convenient to have the quantity nD as one of the basic parameters. A convenient coefficient involving nD to the first power can be obtained by writing

$$C_P{}^{-1/3} = nD\left(\frac{\rho D^2}{P}\right)^{1/3} \tag{1}$$

In figure 1 the propeller selection charts of references 1 and 2 for four- and eight-blade single-rotating propellers have been rearranged as propeller-performance charts to show the optimum induced efficiency η_i as a function of $C_{P_i}{}^{-1/3}$ with $(\sigma c_l)_{0.7R}$ and J as parameters. Also included are lines of constant $P_{c_{v_i}}{}^{-1/3}$ where

$$P_{c_{v_i}}{}^{-1/3} = V\left(\frac{\rho D^2}{P_i}\right)^{1/3} \tag{2}$$

The subscript i denotes that the drag losses are not included.

The induced efficiency η_i and the element loading coefficient $(\sigma c_l)_{0.7R}$ are primarily functions of the power due to lift P_i rather than the total power P, but there is also some dependency on the distribution of lift along the blades. This latter dependency can be ignored in many cases with only a small loss in accuracy. For cases where the propeller operates near peak efficiency, η_i can be considered as dependent on P rather than on P_i as a first approximation with sufficient accuracy for preliminary propeller analyses.

The induced efficiency is dependent upon the number of blades. The results in figure 1, which are for four- and eight-blade propellers, can

be used, however, to determine desirable values of J and $\left(\sigma c_l\right)_{0.7R}$. Once J and $\left(\sigma c_l\right)_{0.7R}$ are determined, η_i can be obtained for the proper number of blades from the propeller selection charts in references 1 and 2, since J and $\left(\sigma c_l\right)_{0.7R}$ are practically independent of the number of blades. The application of the results in figure 1 to propeller-performance problems is illustrated by example performance problems to be given subsequently.

Profile-Drag Losses and Airfoil Data

Profile-drag losses.- For typical thin propellers, reference 3 presents curves of peak profile efficiency η_o as a function of the flight Mach number for various values of J from $J = 2$ to $J = 6$. These curves are reproduced herein as figure 2. When J is less than about 2, it is not a very suitable parameter on which to base curves of peak η_o because the profile efficiency becomes quite dependent on the induced efficiency. Another parameter, however, defined as $J_i = J\left(1 + \frac{1}{2}\bar{w}\right) = \frac{J}{\eta_i}$ has been used to show η_o as a function of flight Mach number, and the results are given in figure 3. The derivation of the results in figure 3 is explained in appendix A.

The results in figures 2 and 3 are based on values of section D/L shown in figure 4. If the maximum L/D at the 0.7R is different from the value used in preparing figures 2 and 3, the approximate value of η_o for the new value of L/D can be obtained from

$$\eta_{o_2} = \frac{\tan\left(\phi + \gamma_1\right)_{0.7R}}{\tan\left(\phi + \gamma_2\right)_{0.7R}} \eta_{o_1} \tag{3}$$

where

$$\left(\tan \phi\right)_{0.7R} = \frac{J_i}{0.7\pi}$$

The values of $\tan \gamma$ at the 0.7R station used for calculating the results in figures 2 and 3 (fig. 4) are reproduced from reference 3.

Airfoil data.- In references 1 and 2, propeller drag losses are expressed in terms of thrust and power coefficients due to drag only ($c_l = 0$). The drag data used in computing these coefficients correspond

[redacted]

to Clark Y airfoil sections for a representative propeller. Inasmuch as the thrust and power coefficients due to drag only are based on the portion of the curve where c_d remains nearly constant when plotted against c_l, it is necessary to ascertain that the propeller is operating with its lift coefficients in this range. This condition is judged by means of propeller design charts which include, among other parameters, values of the element loading coefficient $(\sigma c_l)_{0.7R}$. The parameter $(\sigma c_l)_{0.7R}$ is readily obtained for given operating conditions and hence $c_{l_{0.7R}}$ can be calculated since $\sigma_{0.7R}$ is a known quantity for a given propeller. When it has been determined that the propeller is operating with the lift coefficient at the 0.7R station in the range for which the drag coefficient remains nearly constant, then the thrust and power coefficients due to drag are deemed applicable. The over-all thrust and power coefficients are obtained by adding the thrust and power coefficients due to lift only to the thrust and power coefficients due to drag only, respectively. Values of efficiency obtained by using these coefficients are shown to be in very good agreement with experimental values of the efficiency.

The present paper concerns propellers having much thinner sections than the representative propeller of references 1 and 2. Furthermore, large Mach number changes are likely to be encountered. For this reason it was found convenient to express the drag-loss data in terms of profile efficiency as shown in figures 2 and 3, in such a manner as to include Mach number effects. As mentioned previously, the η_o curves shown are based on typical drag-lift ratios for thin airfoil sections.

Whereas the application of the drag data in references 1 and 2 is restricted to operating lift coefficients in the range where c_d remains nearly constant, the application of the data in figures 2 and 3 is restricted to operating lift coefficients in the range giving maximum or near-maximum L/D. The operating lift coefficients are judged in the same manner as in reference 1. Either the design charts of references 1 and 2 or the performance charts in figure 1 of the present paper can be used for this purpose. It is necessary, however, to have some idea of the range of c_l giving maximum or near-maximum L/D before the results can be applied.

The variation of L/D against c_l with M_x as parameter is shown for the NACA 16-004 and the NACA 16-304 airfoil sections in figures 5 and 6, respectively (data from ref. 4). The results for the NACA 16-004 symmetrical airfoil section (fig. 5) show that, at a given value of M_x, L/D remains near its maximum value over a fairly large range of lift coefficient. At $M_x = 1.0$, for example, L/D varies 10 percent or less

from its maximum value over a c_l range from approximately 0.25 to 0.43. For the NACA 16-304 cambered airfoil section (fig. 6) at $M_x = 1.0$ the c_l range is from 0.37 to 0.61. The range of c_l for which L/D varies 10 percent or less from its maximum value becomes smaller than the ranges shown when M_x is greater than 1.0 and becomes larger when M_x is less than 1.0.

Although the results in figures 2 and 3 are based on maximum L/D values, variations of 10 percent or less from these values have only a small effect on the profile efficiency. In doubtful cases the correction formula expressed in equation (3) can be used. Since the value of $\tan \gamma$ at the 0.7R station used in obtaining the η_o values shown in figures 2 and 3 is given in figure 4, such corrections can be readily applied when different values of $\tan \gamma$ are encountered.

Comparisons of the results in figures 5 and 6 show that the maximum L/D of the cambered section (fig. 6) is higher than the maximum L/D of the symmetrical section (fig. 5) at given section Mach numbers up to about 1.1. It is known, however, that for section Mach numbers above about 1.2, the symmetrical sections have the higher maximum L/D values. When it is desired to estimate propeller performance by the present short method, it is preferable to have airfoil data for the 0.7R station of the particular propeller under consideration. When such data are available, differences between the available data and the data used in preparing figures 2 and 3 can be resolved (eq. (3)).

Figure 7 shows the variation of c_l for maximum L/D as a function of section Mach number. Data used in preparing this figure are from reference 4 for section Mach numbers up to approximately 1.2. For higher Mach numbers the data are calculated for a 4-percent-thick biconvex airfoil having a friction-drag coefficient of 0.006. The lift coefficient for maximum L/D is seen to vary with section Mach number. It will be seen later that performance calculations involve differences in operating conditions between some high-speed design condition and lower-speed climbing and take-off conditions. Since the section Mach number changes accordingly, the variation of c_l for maximum L/D as a function of section Mach number is of some importance. The curve shown (fig. 7) is illustrative and would be expected to vary depending on the airfoil section used.

A complete discussion of airfoil characteristics cannot be given here. The discussion given is intended to present some of the factors which concern the application of the present short method of propeller performance.

[redacted]

Engine Characteristics

The turboengine is the engine which is currently of most interest in regard to application to propeller-driven high-speed airplanes. The operating characteristics of a typical turboengine at full power in terms of the maximum power at static sea-level conditions are shown in figure 8 as a function of airplane speed or Mach number and altitude. At a constant altitude, the full power available increases with increasing velocity up to some "ram power" limit, and at constant velocity, the full power decreases as the altitude is increased.

The quantities of interest in regard to the present analysis are the quantities under the radical $\sqrt[3]{\frac{\rho D^2}{P}}$ since this radical is needed in the calculation of $C_P^{-1/3}$ and $P_{C_v}^{-1/3}$. In order to reduce computational work, the quantity $\left(\frac{\rho_o D^2}{P_o}\right)^{1/3}$ is plotted as a function of horsepower for various diameters in figure 9. Figure 10 gives the quantity $\left(\frac{\rho/\rho_o}{P/P_o}\right)^{1/3}$ as a function of velocity and altitude; this figure is essentially a replot of figure 8. With the static sea-level power, the altitude, the velocity, and the diameter given, then

$$\left(\frac{\rho D^2}{P}\right)^{1/3} = \left(\frac{\rho_o D^2}{P_o}\right)^{1/3}\left(\frac{\rho/\rho_o}{P/P_o}\right)^{1/3} \tag{4}$$

Application of Data

The required steps for estimating the peak efficiency are summarized briefly as follows:

(1) Required data:

(a) P_o

(b) D

(c) $\sigma_{0.7R}$

(d) B

[redacted]

(e) V

(f) Altitude

(g) $c_{l_{0.7R}}$ for maximum L/D as a function of section Mach number

(2) Computational steps:

(a) Obtain $\left(\frac{\rho D^2}{P}\right)^{1/3}$ from figures 9 and 10 by using equation (4) (or engine data if available).

(b) Compute $P_{c_v}^{-1/3} = V\left(\frac{\rho D^2}{P}\right)^{1/3}$.

(c) Compute $(\sigma c_l)_{0.7R}$ by using c_l for maximum L/D and at the intersection of $P_{c_v}^{-1/3}$ and $(\sigma c_l)_{0.7R}$ in figure 1 obtain J.

(Note: This step involves the selection of c_l for maximum L/D without prior knowledge of the section Mach number $M_{0.7R}$ which is given by

$$M_{0.7R} = M\sqrt{1 + \left(\frac{0.7\pi}{J}\right)^2}$$

For airfoil sections where c_l for maximum L/D varies extensively with $M_{0.7R}$, however, these steps may be repeated using trial values of c_l until a value of c_l which is consistent with the corresponding $M_{0.7R}$ is obtained. Exact agreement is not essential inasmuch as η_o remains nearly constant in the range of c_l giving near-maximum L/D.)

(d) With J and $(\sigma c_l)_{0.7R}$ known, obtain η_i. (Note: For four- and eight-blade propellers, η_i can be obtained directly from figure 1. For other numbers of blades, obtain η_i from the propeller selection charts of references 1 and 2.)

[redacted]

(e) Obtain the value of η_o from figure 2 or 3 by using equation (3) if necessary. If J is 2.0 or greater, read η_o from figure 2 for the given flight Mach number and J. If J is less than 2.0, compute $J_i = \frac{J}{\eta_i}$ and obtain η_o from figure 3 for the given flight Mach number M.

(f) Compute $\eta = \eta_i \eta_o$.

(g) Obtain n from either

$$n = \frac{V}{JD}$$

or

$$n = \frac{C_P^{-1/3}}{D\left(\frac{\rho D^2}{P}\right)^{1/3}}$$

where $C_P^{-1/3}$ is obtained from figure 1. The required gear-ratio change can be determined by comparing the new value of n with the original design value.

Static Thrust of Thin Propellers

A method of estimating the static thrust of thin propellers is described in appendix B. The application of this method involves the use of figure 11, which shows curves of C_P and C_T plotted against $(\sigma c_l)_{0.7R}$ with $\frac{\bar{L}}{D} \approx \frac{1}{3}\left(\frac{L}{D}\right)_{0.7R}$ as parameter. (See appendix B regarding limitations.) For cases where C_P, $\sigma_{0.7R}$, and $M_{0.7R}$ are known, the estimation of C_T requires only a curve of L/D against c_l for the airfoil section at the 0.7R station, as shown in figure 5 or 6. The first step in estimating C_T is to plot a curve of $\overline{L/D}$ against $(\sigma c_l)_{0.7R}$ using the data in figure 11 at the required value of C_P. Inasmuch as $\sigma_{0.7R}$ is a given quantity, another curve of $\frac{\bar{L}}{D} = \frac{1}{3}\left(\frac{L}{D}\right)_{0.7R}$ corresponding to the airfoil data can be plotted against $(\sigma c_l)_{0.7R}$.

[redacted]

The intersection of these two curves gives the values of $\overline{L/D}$ and $(\sigma c_l)_{0.7R}$ which are consistent with the given C_P; these values are used to obtain C_T from figure 11.

An alternative method of obtaining the static thrust is provided through the use of figures 12 and 13. Figure 12 shows the ideal thrust T_i (in terms of the density ratio) plotted against the product of the known diameter and power. (See appendix B.) Figure 13 gives the ratio T/T_i as a function of $C_P^{-1/3}$ with $(\sigma c_l)_{0.7R}$ and $\overline{L/D}$ as parameters. When the values of $(\sigma c_l)_{0.7R}$ and $\overline{L/D}$ which give the required value of C_P have been determined, the ratio T/T_i can be obtained directly from figure 13 and the thrust is obtained as the product of T_i and T/T_i.

The ratio T/T_i, as explained in appendix B, is obtained from

$$\frac{T}{T_i} = 0.86 \frac{C_T}{C_P^{2/3}}$$

and is more truly a figure of merit than is the commonly used ratio C_T/C_P.

DISCUSSION

To illustrate the application of the results in figure 1 to propeller-performance problems, consider a four-blade propeller with design conditions such that it operates at $J = 2.5$ and $(\sigma c_l)_{0.7R} = 0.07$. The corresponding values of $C_P^{-1/3}$ and $P_{c_v}^{-1/3}$ are 1.37 and 3.45, respectively (fig. 1). Now consider that it is required to reduce the velocity to one-third of its design value with no change in power, density, or rotational speed. With these quantities fixed, the quantity $C_P^{-1/3}$ remains unchanged from its previous value of 1.37. A new value of $P_{c_v}^{-1/3} = \frac{1}{3} \times 3.45 = 1.15$ has been obtained, however, and the propeller now operates at conditions corresponding to the intersection of the new value of $P_{c_v}^{-1/3}$ and the given value of $C_P^{-1/3}$. This

[redacted]

intersection is beyond the data for four-blade propellers in figure 1(a), but the results for the eight-blade propeller, figure 1(b), indicate that $(\sigma c_l)_{0.7R}$ is approximately 0.215. Inasmuch as σ_{07R} is a fixed quantity, the lift coefficient at the reduced speed is roughly three times its value at the design speed. Hence it is implied that L/D has suffered a drastic reduction from its value at the design condition with serious consequences on the total efficiency.

With variable propeller gearing, however, the quantity $C_P^{-1/3}$ can be changed by changing nD. In this particular problem, $P_{c_v}^{-1/3} = 1.15$ remains constant and the intersection of this line with some desired value of $(\sigma c_l)_{0.7R}$ gives a new value of $C_P^{-1/3}$. For example, it may be desired to operate the propeller with the same value of $(\sigma c_l)_{0.7R}$ at the reduced forward speed as was used at the design forward speed. The intersection of the line $(\sigma c_l)_{0.7R} = 0.07$ and the line $P_{c_v}^{-1/3} = 1.15$ gives a new value of $C_P^{-1/3} = 2.42$. Thus, in order to operate at the desired value of $(\sigma c_l)_{0.7R}$, the rotational speed should be increased in the ratio $\frac{2.42}{1.37} = 1.765$. The induced efficiency now becomes 0.757, or about 8 percent higher than the induced efficiency with single-speed gearing. It is also implied that a reduction in profile-drag losses has been accomplished, since the blade sections now operate nearer their values of c_l for maximum L/D than they did with fixed gearing.

The foregoing example has been offered only as a much simplified version of the application of figure 1 to propeller-performance problems. In actual practice an airplane flying at a small fraction of its design speed is usually at some altitude less than the design altitude and thus the density becomes a variable. The power supplied by the engine may also be a function of flight speed and altitude. Inasmuch as both ρ and P appear in the parameters $P_{c_v}^{-1/3}$ and $C_P^{-1/3}$, it is necessary to evaluate these quantities for each particular operating condition. Finally, in the example problem just considered, a very large increase in rotational speed (over 75 percent) was required to obtain the same value of $(\sigma c_l)_{0.7R}$ at low speed as was used to absorb the given power at the design speed. In a practical case such an increase in rotational

speed (aside from possible structural difficulties) might lead to compressibility losses of the same order of magnitude as the losses due to stalled operation with fixed gearing at the lower rotational speed.

Effect of Altitude Changes and Design Advance Ratio on Propeller-Performance

In the example of the applicability of the results in figure 1 to propeller-performance problems just given, an oversimplified problem was investigated in which the power and density were assumed to remain constant while the airplane velocity was reduced to one-third of its design velocity. Then, if it would be desirable to operate the propeller at the design value of $(\sigma c_l)_{0.7R}$ at this new velocity, it was found that a 76.5-percent increase in rotational speed would be required. It is now assumed that the design conditions, which led to a design advance ratio of 2.5 with $(\sigma c_l)_{0.7R} = 0.07$, correspond to an altitude of 40,000 feet. The quantities $C_P^{-1/3}$ and $P_{c_v}^{-1/3}$ have the same values as before; that is, $C_P^{-1/3} = 1.37$ and $P_{c_v}^{-1/3} = 3.45$. Now assume that the propeller is to be operated at sea level at one-fourth of its design velocity with no change in engine power or rotational speed. Under these conditions

$$C_{P_2}^{-1/3} = \left(\frac{\rho}{\rho_o}\right)^{-1/3} C_{P_1}^{-1/3} = 2.19$$

and

$$P_{c_{v_2}}^{-1/3} = \frac{1}{4}\left(\frac{\rho}{\rho_o}\right)^{-1/3} P_{c_{v_1}}^{-1/3} = 1.38$$

From figure 1, the value of $(\sigma c_l)_{0.7R}$ corresponding to these new values of $C_P^{-1/3}$ and $P_{c_v}^{-1/3}$ is about 0.077 with $\eta_i = 0.808$. If $c_{l_{0.7R}}$ for maximum L/D remains approximately constant with section Mach number, it is evident that variable gearing is not needed, because the rotational speed remains near optimum for both the design speed and altitude and for the reduced speed and reduced altitude.

[redacted]

One more case is investigated before extending the discussion to include Mach number effects. In this case the design conditions are such that the propeller operates at 40,000 feet altitude with $J = 4.0$ and $(\sigma c_l)_{0.7R} = 0.07$. The corresponding values of $C_P^{-1/3}$ and $P_{C_v}^{-1/3}$ are respectively 1.05 and 4.20. If this propeller is operated at sea level at one-fourth of the design velocity with no change in rotational speed and power, the new values of $P_{C_v}^{-1/3}$ and $C_P^{-1/3}$ become

$$C_{P_2}^{-1/3} = \left(\frac{\rho}{\rho_o}\right)^{-1/3} C_{P_1}^{-1/3} = 1.68$$

$$P_{C_{v_2}}^{-1/3} = \frac{1}{4}\left(\frac{\rho}{\rho_o}\right)^{-1/3} P_{C_{v_1}}^{-1/3} = 1.68$$

With these new values, the operating value of $(\sigma c_l)_{0.7R}$ (from fig. 1) is approximately 0.115. Hence for this case a change in gear ratio might be desirable because of the increase in operating lift coefficient corresponding to the change in σc_l from 0.07 at altitude to 0.115 at sea level.

The foregoing examples have served to show that the propeller performance is dependent on a large number of variables. Inasmuch as some of these variables are subject to arbitrary control depending on the desired flight plan, a general performance investigation does not appear feasible. The ultimate in propeller performance would probably require, in addition to the continuously variable blade-angle changing mechanism which is currently available, a continuously variable gear-ratio changing mechanism. Such a mechanism suitable for use on airplanes has not been developed. A two-speed gear-ratio mechanism is relatively simple in application, however, and a sample performance problem is analyzed to show some of the cases where the application of a two-speed gear ratio mechanism might serve to increase the take-off performance of a propeller-driven airplane.

Example Performance Problem

Efficiency at take-off.- The following example problem is based on the characteristics of a turboengine which produces 9,000 shaft horsepower at static sea-level conditions. The variation of full power with

changes in velocity and altitude corresponds to the changes shown in figure 8. The jet thrust produced by the engine is not considered in the present problem.

The design altitude will be taken as 40,000 feet with the design Mach number equal to 0.9. It is first necessary to select propellers to meet the design requirements. As a first step in the propeller selection, the blades will be assumed to have the thickness distribution and the airfoil characteristics of the "thin" propeller of reference 3. The previous brief analysis of variable gearing indicated that variable gearing might or might not be required for optimum low-speed performance in the take-off range depending on the design advance ratio. Hence a series of propellers with the design advance ratio varying from 2 to 4 will be investigated. The diameter and number of blades is selected in an arbitrary manner. The propellers are to be used on a bomber-type airplane having a wing loading of 60 pounds per square foot.

Propellers which are suitable for the design conditions are listed in table I.

Assuming that the airplane $\left(\frac{W}{S} = 60\right)$ takes off at sea level with $C_L = 1.2$, the velocity at take-off is 205 feet per second ($M_{TO} = 0.184$). For each design advance ratio and diameter, table II lists the value of J_{TO} with fixed gearing and the approximate value of $(\sigma c_l)_{0.7R}$ which would be required to absorb 9,000 horsepower at the given rotational speed. The steps involved in obtaining $(\sigma c_l)_{0.7R}$, and $M_{0.7R}$ are also indicated.

The results in table II show that the required value of $(\sigma c_l)_{0.7R}$ for take-off with fixed gearing is in all cases higher than the design value of $(\sigma c_l)_{0.7R}$ for high speed. The required increase in $c_{l_{0.7R}}$ for take-off becomes larger as the design advance ratio increases. The required increase varies from a factor of about 1.65 for the low-design-advance-ratio propeller to about 3.0 for the high-design-advance-ratio propeller.

For the propeller with the design advance ratio of 2.0, the section Mach number at 0.7R is 1.337 at high speed. From figure 7 the operating c_l for maximum L/D at this Mach number is about 0.25. At take-off with fixed gearing the section Mach number is reduced to 0.91 (table II). At this Mach number the value of c_l for maximum L/D is about 0.35. Thus, to operate at maximum L/D at take-off, the high-speed values of

$(\sigma c_l)_{0.7R}$ should be increased by a factor $\frac{0.35}{0.25} = 1.4$ rather than in the ratio 1.65 actually obtained with fixed gearing. Since the value of $c_{l_{0.7R}}$ with fixed gearing (0.41) is very near the value of c_l (0.35) for maximum L/D, it is probable that two-speed gearing would produce no significant gain in take-off performance for the low-advance-ratio propellers. The approximate efficiency of these propellers is given subsequently.

The values of $(\sigma c_l)_{0.7R}$ required for take-off with fixed gearing for the propellers having design advance ratios of three or four are much higher than the high-speed values (tables I and II), whereas for best efficiency the values should be nearly the same as for high speed. Inasmuch as the tip speeds are relatively low with fixed gearing, the efficiency can be estimated by means of existing propeller test data because moderate differences in propeller thickness are relatively unimportant at low section speeds.

The efficiency at take-off for the various propellers with fixed gearing and with two-speed gearing is shown in table III. The efficiency with fixed gearing for the propellers having design J equal to 3 and 4 is estimated from experimental results for the NACA 10-(3) (08)-03-45 propeller in reference 5. The other efficiencies are estimated by means of figures 1 and 3. The desired values of $(\sigma c_l)_{0.7R}$ for take-off for the $J = 2.0$ propellers are the values shown in table II. The desired values for the other propellers are taken to be the same as for high speed (table I).

The results in table III show that a considerable increase in take-off efficiency results from the use of two-speed gearing for the propellers having design advance ratios of 3.0 or greater. This gain is about 10 to 15 percent when $J = 3.0$ and the gain is about 20 to 30 percent when $J = 4.0$. The efficiencies at take-off of the propellers having $J = 3.0$ with two-speed gearing are about 7 percent higher than the efficiencies at take-off for the propellers having $J = 2.0$. The take-off efficiencies with two-speed gearing for the propellers having $J = 4.0$ are about 15 percent higher than for the propellers having $J = 2.0$.

In this particular example the take-off efficiencies of the propellers having a design advance ratio of 2.0 are 60 percent or better, and thus the propellers should be adequate for many purposes although not quite so efficient as the larger propellers turning at their optimum rotational speeds. A point in favor of the low-design-advance-ratio propeller is that a relatively high take-off efficiency is obtained without the complications of two-speed gearing. A point in favor of the

propellers having $J = 4.0$, however, is that higher take-off efficiencies are obtained with lower centrifugal stresses than those which occur with low design advance ratios.

Static thrust.- The approximate static thrusts of the example propellers operating at their optimum rotational speeds for take-off are shown for comparison with the static thrusts obtainable with fixed gearing in table IV.

In table IV the values of T/T_i corresponding to the optimum rotational speed for take-off were obtained from figures 11 and 13 by the previously explained method of cross-plotting. The airfoil characteristics for the 0.7 radius station correspond to the data for the NACA 16-304 airfoil section in figure 6. The use of symmetrical airfoil sections would result in somewhat lower values of T/T_i (see appendix C). The values of T/T_i with fixed gearing (except for the propellers having $J = 2.0$) were estimated from tests results for the NACA 4-(3)(08)-03 propeller and may be somewhat high because of the greater thickness. Values of T_i are from figure 12.

The results in table IV show that a large gain in static thrust is obtainable through the use of variable gearing for the propellers having design advance ratios of 3.0 and 4.0. The importance of having as large a diameter as possible is also shown. The diameter becomes of secondary importance, however, when the take-off speed has been obtained (see table III), although an advantage remains with the larger-diameter propeller of a given design advance ratio.

It should be kept in mind that the analysis just given applies to a particular set of design conditions. Hence, in general, the use of variable-speed gearing will not necessarily permit propeller operation at peak efficiency at take-off, nor will it always be possible to determine a compromise design advance ratio such that peak or near-peak take-off efficiency will occur without variable gearing. Each performance problem must be examined in the light of the pertinent design variables.

CONCLUDING REMARKS

From the standpoint of propeller performance, the aerodynamic problem is simply to determine whether or not the propeller is operating with optimum lift-coefficient values at a given forward speed, rotational speed, and power. Optimum values of section lift coefficient are values producing maximum or near-maximum lift-drag ratios. The operating lift coefficient at the 0.7 radius station is a fair measure of the over-all

[redacted]

operating conditions, and the charts in the present paper permit a rapid estimation of this value for given speeds and powers when the solidity is known. From the standpoint of efficiency, the two-speed gearing problem is simply to determine the change in rotational speed necessary to obtain optimum section lift coefficient for cases where nonoptimum values are encountered when using fixed gearing; this change is readily estimated through the use of the performance charts. More precise evaluation of required rotational-speed changes will probably require experimental data on thin propellers.

In an example performance problem involving the application of several different propellers to a given set of design conditions, analysis of the take-off problem shows that the take-off performance is dependent upon the design advance ratio at high speed. With a design advance ratio of 2.0, peak efficiency at take-off occurs at very nearly the same rotational speed required for high speed. With a design advance ratio of 3.0 or 4.0, the propellers operate with values of section lift coefficient well beyond the value for maximum lift-drag ratio; this tendency toward stalled operation increases progressively with increases in the design advance ratio. By using two-speed gearing to operate with optimum values of section lift coefficient, however, the performance at take-off of the higher-design-advance-ratio propellers is superior to that of the lower-design-advance-ratio propellers. This superiority is quite pronounced at static thrust.

A brief analysis of the peak static thrust of thin-blade propellers shows that moderately cambered propellers produce up to 20 percent more thrust than do propellers incorporating symmetrical blade sections. At rotational tip Mach numbers in excess of about 1.2, there is a substantial drop in peak static thrust.

Langley Aeronautical Laboratory,
National Advisory Committee for Aeronautics,
Langley Field, Va.

[redacted]

APPENDIX A

METHOD OF CALCULATING PROFILE EFFICIENCY

The propeller element efficiency is

$$\eta' = \frac{V dT}{dP}$$

where.

$$dT = \frac{1}{2} \rho W^2 Bb \left(c_l \cos \phi - c_d \sin \phi\right) dr$$

and

$$dP = 2\pi rn \frac{1}{2} \rho W^2 Bb \left(c_l \sin \phi + c_d \cos \phi\right) dr$$

By taking $x = \frac{r}{R}$, introducing from reference 6

$$bc_l = \frac{(V + w)w}{Bn} K(x) \frac{2 \sin \phi}{V + \frac{1}{2} w \cos^2 \phi}$$

$$W = \frac{1}{\sin \phi}\left(V + \frac{1}{2} w \cos^2 \phi\right)$$

and integrating to get

$$\eta = \frac{V \int_{x_o}^{1.0} \frac{dT}{dx} dx}{\int_{x_o}^{1.0} \frac{dP}{dx} dx}$$

[redacted]

the result becomes, for the optimum case where the induced efficiency remains constant with radius,

$$\eta = \eta_i \frac{\int_{x_o^2}^{1.0} \left(1 + \frac{1}{2}\bar{w}\cos^2\phi\right)K(x)(1 - \tan\phi\tan\gamma)d(x^2)}{\int_{x_o^2}^{1.0} \left(1 + \frac{1}{2}\bar{w}\cos^2\phi\right)K(x)(1 + \cot\phi\tan\gamma)d(x^2)}$$

Inasmuch as ϕ, $K(x)$, and η_i are determinable for given values of J when the parameter $\frac{1}{2}\bar{w}$ is specified, solutions of the foregoing equation would be obtained readily if values of $\tan\gamma$ were given. Peak values of η would in general be obtained if the values of $\tan\gamma$ corresponded to maximum values of L/D at the appropriate section Mach number. Since the maximum L/D is a function of the section Mach number, which in turn is a function of J and M, it would be possible to show approximate values of peak η with $\frac{1}{2}\bar{w}$, J, and M as parameters. Typical values of peak η could be shown as functions of J and M by a series of charts. There would be one chart for each value of $\frac{1}{2}\bar{w}$.

It is shown in reference 6 by a somewhat different approach that, because of obvious uncertainties in the determination of c_d (or the value of $\tan\gamma$ corresponding to maximum L/D in the present case), it is not necessary to retain the term $\frac{1}{2}\bar{w}\cos^2\phi$. Several trial calculations, in which the term $\frac{1}{2}\bar{w}\cos^2\phi$ was retained and dropped in turn, showed that the ratio of the terms under the integral signs of the present equation has only a slight dependency on $\frac{1}{2}\bar{w}\cos^2\phi$. This term can therefore be dropped with only a slight loss in accuracy. With this simplification the expression for η can be written

$$\eta = \eta_i \frac{\int_{x_o^2}^{1.0} K(x)(1 - \tan\phi\tan\gamma)d(x^2)}{\int_{x_o^2}^{1.0} K(x)(1 + \cot\phi\tan\gamma)d(x^2)}$$

$$= \eta_i \eta_o$$

[redacted]

It is now possible to show approximate values of η_o as a function of J and M on a single chart by the following method.

From reference 6 the aerodynamic helix angle is given by

$$\tan \phi = \frac{J(1 + \frac{1}{2}\bar{w})}{\pi x}$$

Inasmuch as

$$\eta_i = \frac{1}{1 + \frac{1}{2}\bar{w}}$$

the aerodynamic helix angle becomes

$$\phi = \tan^{-1} \frac{J}{\eta_i} \frac{1}{\pi x}$$

By defining

$$J_i = \frac{J}{\eta_i}$$

the quantity J_i becomes a measure of the aerodynamic helix angles in the same manner that J is a measure of the geometric helix angles. Another definition of J_i is

$$J_i = J\left(1 + \frac{1}{2}\bar{w}\right)$$

By using J_i as a parameter to obtain values of $K(x)$ (rather than the more exact expression $J(1 + \bar{w})$) and also by obtaining values of section Mach number from the approximate relation

$$M_x \approx M\sqrt{1 + \left(\frac{\pi x}{J_i}\right)^2}$$

[redacted]

the equation for η_o was solved for various values of J_1 and M using values of $\tan \gamma$ corresponding to the thin propeller of reference 4. The results are given in figure 3. The results in figure 3 are approximately correct when the propeller operates at or near the c_l value for maximum L/D at the 0.7R station.

APPENDIX B

STATIC THRUST

The ratio C_T/C_P, commonly called the static-thrust figure of merit, is usually employed when presenting propeller static-thrust data, and some methods of analysis of propeller static-thrust performance involve the use of this ratio. It is very difficult, however, to visualize the performance of a given propeller when C_P, and therefore C_T/C_P, becomes a variable as it does when variable gearing is considered.

A more useful static-thrust figure of merit is the ratio of the static thrust of a given propeller to the static thrust of an actuator disk of the same diameter for a given power. In reference 7, Bairstow gives relations for the static thrust and power of an actuator disk as

$$T_i = \rho\pi \frac{D^2}{4} \frac{u^2}{2}$$

and

$$P = \frac{1}{4} \rho\pi \frac{D^2}{4} u^3$$

By solving for u in terms of P and substituting in the equation for thrust, the following equation can be obtained:

$$T_i = \left(\frac{\rho}{\rho_o}\right)^{1/3} (0.0612DP)^{2/3}$$

The quantity T_i is the highest thrust possible for a given density, power, and diameter where axial losses only are considered. It can be shown that

$$\frac{T}{T_i} = 0.86 \frac{C_T}{C_P^{2/3}}$$

[redacted]

where C_T and C_P are experimental values or calculated values including all losses. Thus the equation expresses the thrust as a fraction of the ideal thrust.

For cases involving the determination of two-speed gearing requirements, it is advantageous to plot the ratio T/T_i as a function of $C_P^{-1/3}$ with M_R as parameter. An example of such a plot is given in figure 14. Data used in preparing figure 14 are experimental data from reference 8 for the NACA 10-(5)(066)-03 two-blade propeller. Given an initial value of M_R and $C_P^{-1/3}$, it is a simple matter to find the effect of changes in nD on the value of T/T_i because both $C_P^{-1/3}$ and M_R change in direct proportion to changes in nD as long as ρ, D, and P remain constant. For example, assume that the NACA 10-(5)(066)-03 two-blade propeller (fig. 14) operates with $C_P^{-1/3} = 2.7$ and $M_R = 0.8$. The value of T/T_i is 0.65. Increasing the rotational speed by 25 percent increases $C_P^{-1/3}$ to 3.377 and $M_R = 1.0$. The new value of T/T_i from figure 14 is 0.74. The increase in static thrust is almost 14 percent.

Experimental values of C_T and C_P at $J = 0$ are often lacking but the conventional vortex propeller theory can be used to determine approximate values of these coefficients by assuming the Betz optimum loading distribution to apply to the static conditions and by making suitable estimates of the profile-drag loss. For the Betz condition

$$x \tan \phi = \text{Constant}$$

With

$$\tan \alpha_i = \frac{\sigma c_l}{4G \sin \phi} = (\tan \phi)_{J=0}$$

the values σc_l and ϕ are determinable for any radius when σc_l is specified for a given radius and number of blades for the propeller. In the present paper this simplification along with the additional simplification that L/D is constant along the blade was used to calculate

$\frac{dC_T}{dx}$ and $\frac{dC_Q}{dx}$ by the method of reference 9 for several given values of $(\sigma c_l)_{0.7R}$ and L/D. These values were integrated from the 0.3R station to the tip to obtain C_T and C_P for four-blade single-rotating propellers. The results are shown plotted in figure 11 with the radially constant value of L/D designated as $\overline{L/D}$.

It is necessary to relate the results in figure 11 to actual operating conditions. A correlation can be found in the following manner. Inasmuch as the element loading coefficient $(\sigma c_l)_{0.7R}$ is a measure of the propeller operating lift coefficients, the results in figure 11 show that C_T is primarily a function of the lift coefficients with only a secondary dependency on the propeller L/D, which is exemplified in this case by $\overline{L/D}$. Hence, given an experimental value of C_T, the approximate $(\sigma c_l)_{0.7R}$, and thus $c_{l_{0.7R}}$ since $\sigma_{0.7R}$ is known, is obtainable at once from figure 11. Then, if airfoil data are given for the airfoil section at the 0.7R station, it is possible to obtain the two-dimensional value of L/D corresponding to $c_{l_{0.7R}}$. At the same time, the intersection of the experimental value of C_P with $(\sigma c_l)_{0.7R}$ (the same $(\sigma c_l)_{0.7R}$ corresponding to experimental value of C_T) in figure 11 gives the value of $\overline{L/D}$.

This procedure was applied to experimental data for several different propellers under various loading conditions and it was found that L/D was related to $(L/D)_{0.7R}$ by an empirical factor

$$\frac{\bar{L}}{D} \approx \frac{1}{3}\left(\frac{L}{D}\right)_{0.7R}$$

With this empirical factor fairly well established, and if two-dimensional airfoil data are given for the airfoil section at the 0.7R station, it is possible to estimate the propeller characteristics at static thrust for given values of C_P, $\sigma_{0.7R}$, and $M_{0.7R}$ by trial and error or by cross-plotting. For each trial value of $c_{l_{0.7R}}$ there is a corresponding value of $\frac{L}{D}_{0.7R}$ and thus $\overline{L/D}$. This combination of $c_{l_{0.7R}}$, expressed as $(\sigma c_l)_{0.7R}$, and $\overline{L/D}$ gives a value of C_P. When

[redacted]

the proper combination which gives the required value of C_P has been obtained, the value of C_T corresponding to $(\sigma c_l)_{0.7R}$ is obtained at once from figure 11.

This method fails at very low blade angles where the outer sections produce negative thrust (a condition of only small interest). The method works reasonably well, however, up into the stalled range of operation. Check strip calculations in appendix C with $M_R = 1.2$ indicate that the method is reasonably accurate at high tip Mach numbers for propellers of small camber ($c_{l_d} = 0.3$ or less). The factor 1/3 used in obtaining $\overline{L/D}$ is reasonably accurate for single-rotating propellers of three or more blades. For two-blade propellers this factor should be reduced by about 10 percent.

For convenience the data of figure 11 are replotted in figure 13 to show the ratio T/T_i as a function of $C_P^{-1/3}$, for various values of $(\sigma c_l)_{0.7R}$ and $\overline{L/D}$. By converting the previously mentioned specified value of C_P to $C_P^{-1/3}$, figure 13 may be used to obtain the ratio T/T_i directly.

It should be pointed out that although the ratio T/T_i is convenient for investigating gear-ratio requirements for a given propeller, allowances must be made for comparisons of propellers of different diameters absorbing a given power. Different diameters give different values of T_i for a given power and density.

APPENDIX C

EFFECT OF CAMBER ON STATIC THRUST

The results in figure 13 show the dependence of the static thrust on L/D of the section. Since camber is one of the variables affecting L/D, it is of interest to make a brief investigation of the effect of camber on the peak static-thrust performance of thin propellers.

The effect of camber on maximum L/D as a function of section Mach number is shown in figure 15 for the NACA 16-004, NACA 16-304, and NACA 16-504 airfoils (data from ref. 4). This figure shows that at subcritical section Mach numbers the cambered sections produce maximum L/D values which are up to three times as high as the maximum L/D for the symmetrical section having the same thickness ratio. When the force-break Mach number is exceeded, however, there is a sharp drop in maximum L/D and eventually the maximum L/D of the NACA 16-504 section becomes lower than the L/D values for the sections of moderate or zero camber.

The airfoil data in reference 4 indicate that, for the section Mach number range under consideration, the lift coefficient for maximum L/D remains approximately constant at 0.40, 0.45, and 0.60 for the NACA 16-004, NACA 16-304, and NACA 16-504 airfoil sections, respectively. The foregoing information on c_l and L/D permits the estimation from figure 13 of peak values of T/T_i as a function of M_R provided that information on the solidity $\sigma_{0.7R}$ is given. Figure 16 is a plot of T/T_i against M_R for three propellers, each of which is assumed to have $\sigma_{0.7R} = 0.16$ but with the camber varying in accordance with the NACA 16-series airfoils just discussed.

According to the results in figure 16, peak values of T/T_i for thin propellers are only slightly affected by compressibility up to a rotational tip Mach number of about 1.2. At $M_R = 1.0$ the data indicate that using NACA 16-504 airfoil sections instead of NACA 16-004 airfoil sections increases the ratio T/T_i from 0.67 to 0.85. At $M_R = 1.2$ a propeller having NACA 16-304 airfoil sections has a peak ratio T/T_i of 0.76 as compared to 0.66 for symmetrical sections. In terms of thrust per horsepower at sea level, a 16-foot-diameter four-blade propeller with $\sigma_{0.7R} = 0.16$ and absorbing 10,000 horsepower at $M_R = 1.2$ would produce a maximum of approximately 2 pounds of thrust per horsepower with symmetrical airfoil sections.

[redacted]

With the NACA 16-304 sections, the same propeller would produce about 2.3 pounds per horsepower, a gain of 15 percent in thrust.

As M_R exceeds a value of about 1.2, the peak values of T/T_i become progressively lower (fig. 16), and it is seen that camber becomes less effective in increasing the static thrust.

Inasmuch as the factor 1/3 used in estimating $\overline{L/D}$ was obtained from low-speed propeller data, check calculations of peak values of T/T_i using strip theory have been made for a rotational tip Mach number of 1.2. The calculations were made for four-blade propellers which were assumed to be rectangular in plan form with $\sigma_{0.7R} = 0.16$. The blades incorporated constant camber corresponding to the camber used in the approximate calculations and were of constant thickness with $\frac{h}{b} = 0.04$. The pitch distribution under load was assumed to correspond to

$$\tan \beta = \frac{J}{\pi x}$$

with $J = 2.0$.

A few trial blade-angle settings were required to arrive at the peak values of T/T_i. For the propellers with $c_{l_d} = 0$ and 0.3, these more realistic values of T/T_i were only 2 or 3 percent lower than the estimated values shown in figure 16 at $M_R = 1.2$. The peak value of T/T_i for the check propeller having $c_{l_d} = 0.5$ was the same as the peak value for the check propeller having $c_{l_d} = 0.3$ and thus was considerably below the estimated value shown in figure 16. This latter disagreement is not considered as serious, however, inasmuch as a value of c_{l_d} of 0.5 for low-advance-ratio propellers is probably excessive from high-speed considerations.

This brief study of camber effects has indicated the desirability of incorporating a moderate amount of camber to obtain good static-thrust performance. More research is needed, however, in order to determine the effects of camber on the over-all propeller performance.

[redacted]

REFERENCES

1. Crigler, John L., and Talkin, Herbert W.: Charts for Determining Propeller Efficiency. NACA ACR L4I29, 1944.

2. Crigler, John L., and Jaquis, Robert E.: Propeller-Efficiency Charts for Light Airplanes. NACA TN 1338, 1947.

3. Gilman, Jean, Jr., Crigler, John L., and McLean, F. Edward: Analytical Investigation of Propeller Efficiency at High-Subsonic Flight Speeds Near Mach Number Unity. NACA RM L9L05a, 1950.

4. Enos, L. H., and Borst, H. V.: Propeller Performance Analysis. Aerodynamic Characteristics, NACA 16 Series Airfoils. Pts. I and II. Rep. No. C-2000, Curtiss-Wright Corp., Propeller Div. (Caldwell, N. J.), Dec. 2, 1948.

5. Gilman, Jean, Jr.: Wind-Tunnel Tests and Analysis of Three 10-Foot-Diameter Three-Blade Tractor Propellers Differing in Pitch Distribution. NACA ARR L6E22, 1946.

6. Crigler, John L.: Application of Theodorsen's Theory to Propeller Design. NACA Rep. 924, 1949. (Supersedes NACA RM L8F30.)

7. Bairstow, Leonard: Applied Aerodynamics. Second ed., Longmans, Green and Co., 1939, p. 628.

8. Wood, John H., and Swihart, John M.: The Effect of Blade-Section Camber on the Static Characteristics of Three NACA Propellers. NACA RM L51I28, 1952.

9. Crigler, John L.: Comparison of Calculated and Experimental Propeller Characteristics for Four-, Six-, and Eight-Blade Single-Rotating Propellers. NACA ACR 4B04, 1944.

[redacted]

TABLE I

EXAMPLE TURBOPROPELLERS

[M, 0.9; altitude, 40,000 ft; P, 4860 hp]

Design J	$\sigma_{0.7R}$	$c_{l_{0.7R}}$	$(\sigma c_l)_{0.7R}$	B	D	η_i	η_o	η	πnD	$M_{0.7R}$
2	0.24	0.25	0.06	3	15.04	0.930	0.820	0.762	1374	1.337
2	.32	.25	.08	4	12.95	.918	.820	.752	1374	1.337
3	.16	.50	.08	4	17.55	.918	.835	.767	916	1.116
3	.24	.50	.12	6	14.20	.902	.835	.753	916	1.116
4	.16	.50	.08	4	21.30	.910	.845	.769	687	1.027
4	.24	.50	.12	6	17.34	.892	.845	.754	687	1.027
4	.32	.50	.16	8	15.04	.870	.845	.735	687	1.027

[redacted]

TABLE II

VALUES OF J_{TO} AND $(\sigma c_l)_{0.7R}$ AT TAKE-OFF WITH FIXED GEARING FOR PROPELLERS OF TABLE I

[V_{TO}, 205 ft/sec; P, 9000 hp; altitude, sea level; $\frac{W}{S}$, 60 lb/sq ft; airplane C_L, 1.2]

Design J	D	J_{TO}	$\left(\frac{\rho_o D^2}{\rho_o}\right)^{1/3}$	$P_{c_v}{}^{-1/3}$	$C_P{}^{-1/3}$	$(\sigma c_l)_{0.7R}$	$M_{0.7R}$	$(\sigma c_l)_{0.7R}$ for high speed
2	15.04	0.469	0.00477	0.978	2.088	0.100	0.91	0.06
2	12.95	.469	.00432	.886	1.890	.130	.91	.08
3	17.55	.703	.00527	1.081	1.538	[a].180	.622	.08
3	14.20	.703	.00460	.943	1.342	[a].250	.622	.12
4	21.30	.938	.00603	1.236	1.318	[a].240	.482	.08
4	17.34	.938	.00525	1.076	1.148	[a].350	.482	.12
4	15.04	.938	.00477	.978	1.043	[a].430	.482	.16

[a]These values are obtained from eight-blade propeller chart, figure 1(b).

TABLE III

EFFICIENCY AT TAKE-OFF

[Propellers of table I]

Design J	D	Fixed gearing		Two-speed gearing	
		η	πnD	η	πnD
2	15.04	0.632	1374	-----	----
2	12.95	.606	1374	-----	----
3	17.55	.590	916	0.680	1370
3	14.20	.580	916	.642	1328
4	21.30	.550	687	.724	828
4	17.34	.540	687	.714	848
4	15.04	.570	687	.694	882

[redacted]

TABLE IV

APPROXIMATE STATIC THRUST AT SEA LEVEL OF PROPELLERS LISTED IN TABLE I, WITH AND WITHOUT TWO-SPEED GEARING

Design J	D	T/T_i		T_i	T	
		Two-speed gear	Fixed-speed gear		Two-speed gear	Fixed-gear
2	15.04	-----	0.760	27,500	------	20,900
2	12.95	-----	.765	25,100	------	19,200
3	17.55	0.725	.450	31,000	22,500	14,000
3	14.20	.760	.450	26,600	20,200	12,000
4	21.30	.740	.350	35,000	25,900	12,250
4	17.34	.755	.350	30,600	23,100	10,700
4	15.04	.750	.350	27,500	20,600	9,600

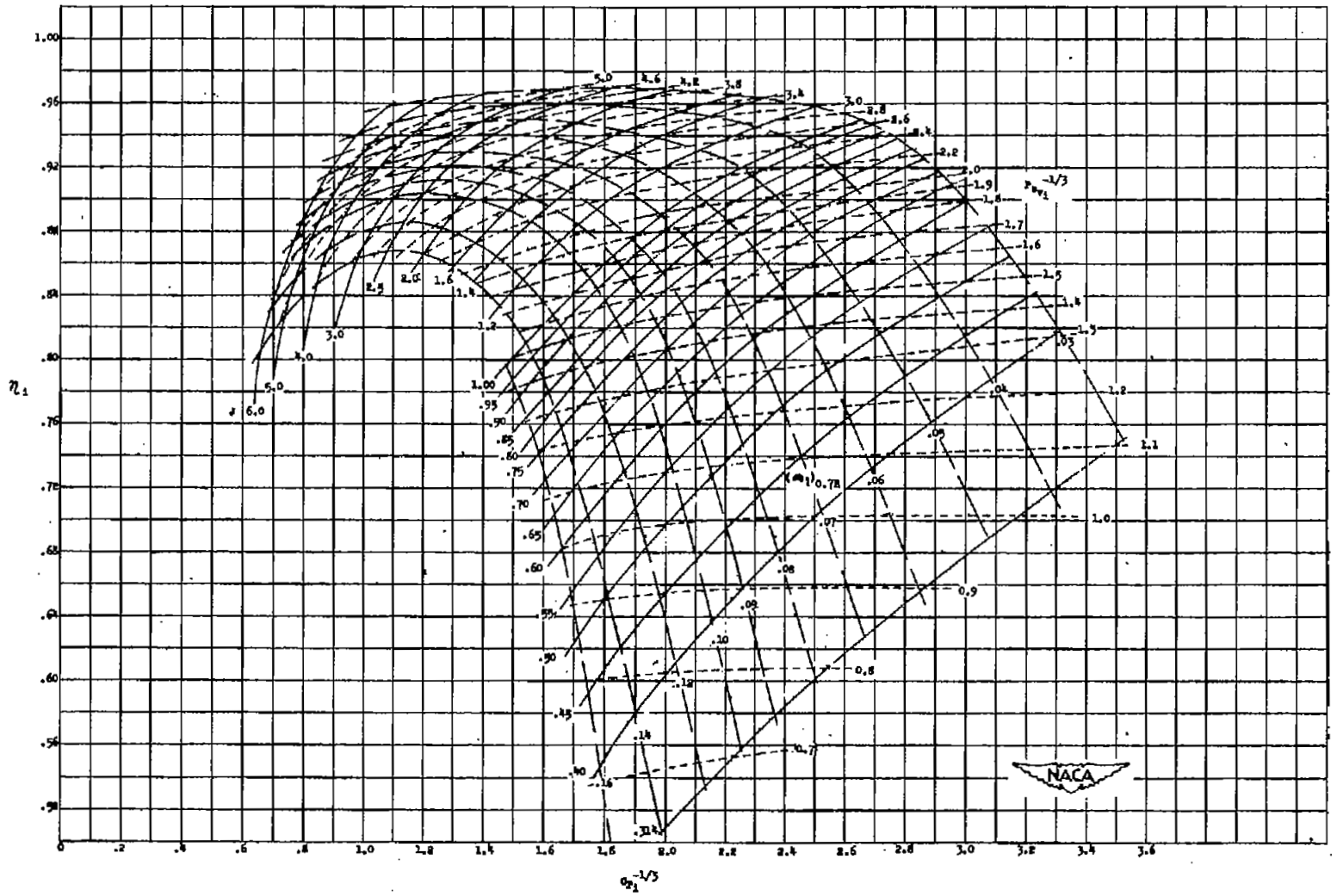

(a) Four-blade propellers.

Figure 1.- Propeller performance charts. Without drag.

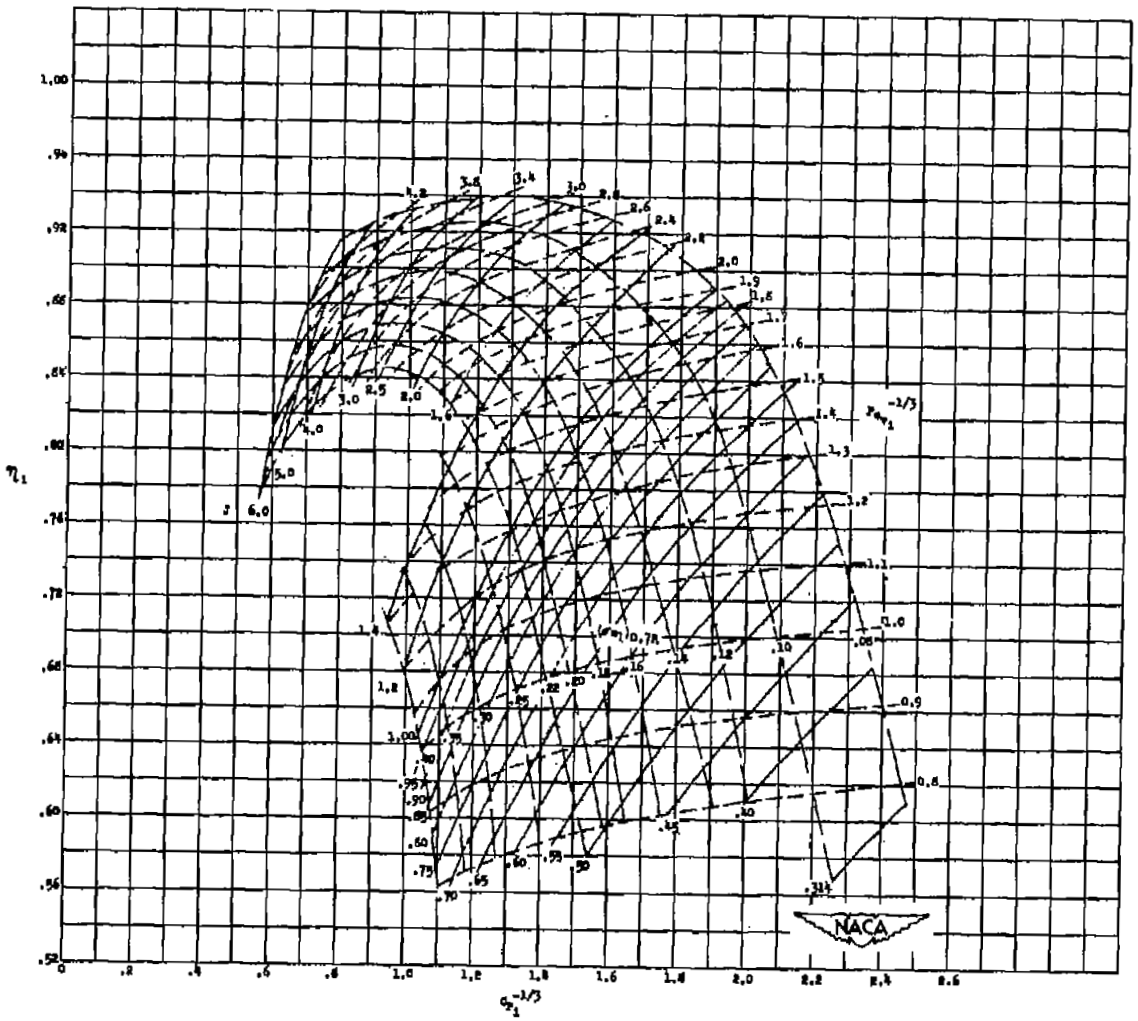

(b) Eight-blade propellers.

Figure 1.- Concluded.

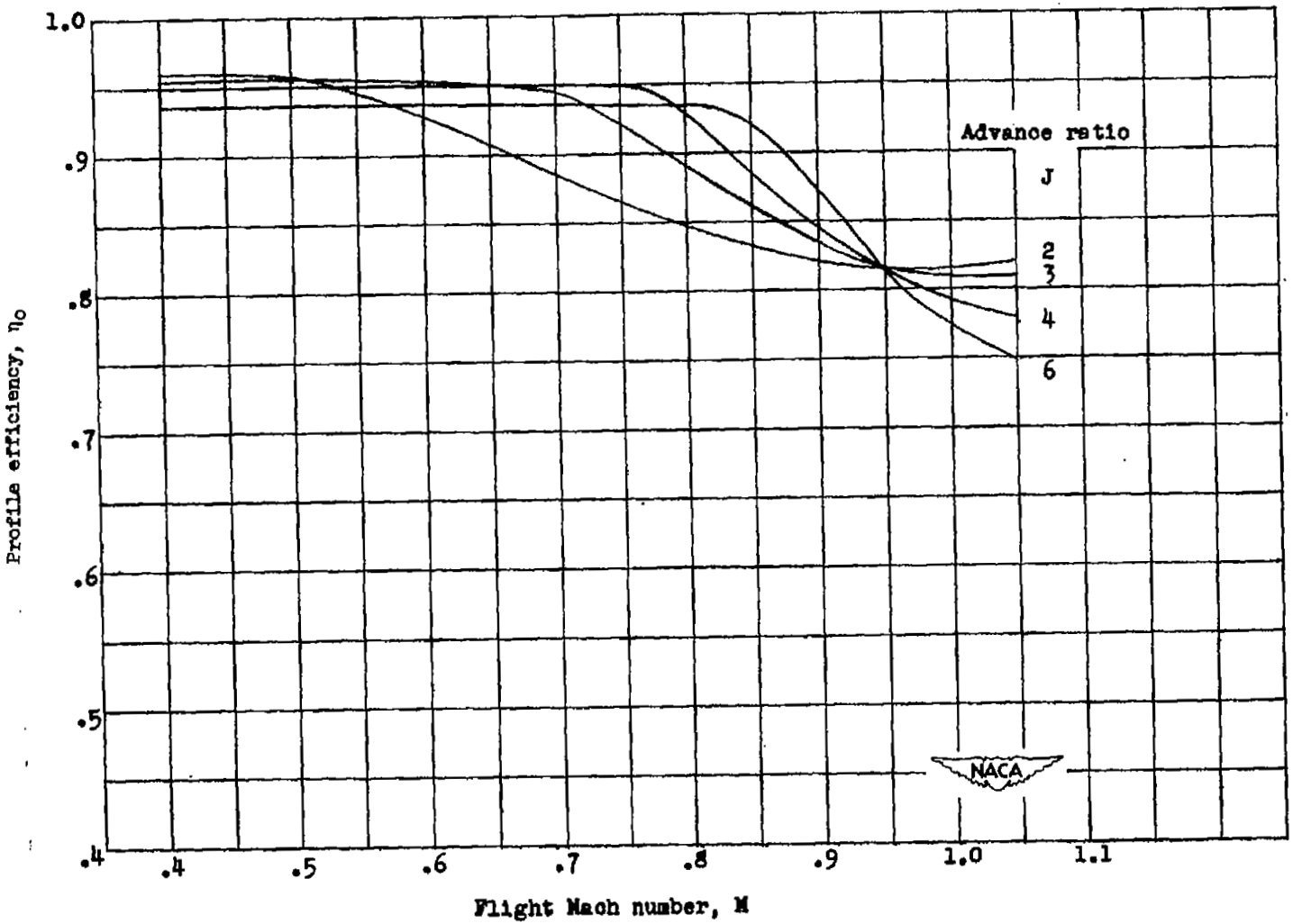

Figure 2.- Peak profile efficiency against flight Mach number for various advance ratios. Thin propellers of reference 3.

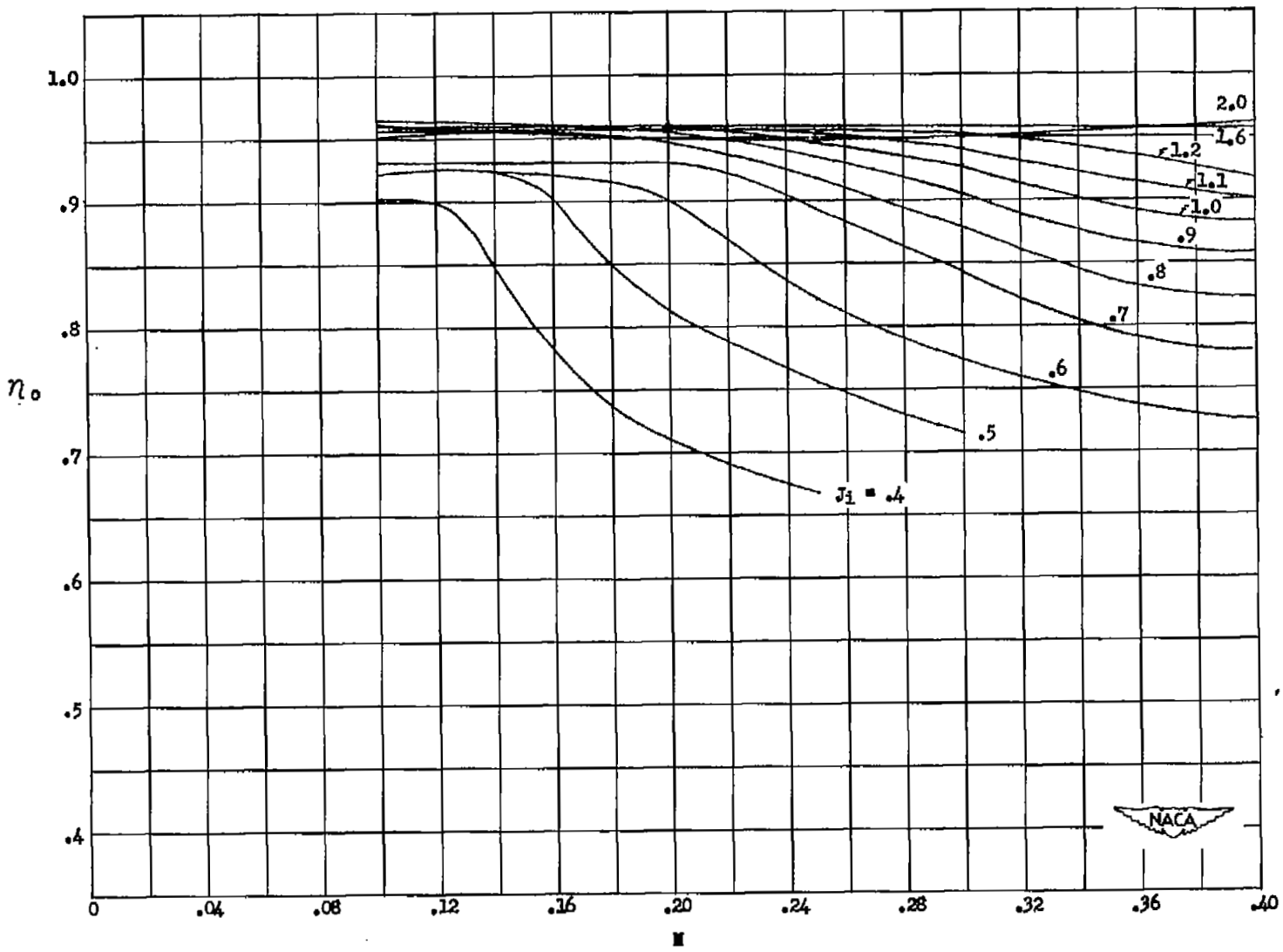

Figure 3.- Profile efficiency as a function of flight Mach number in the take-off range. Thin propellers of reference 3.

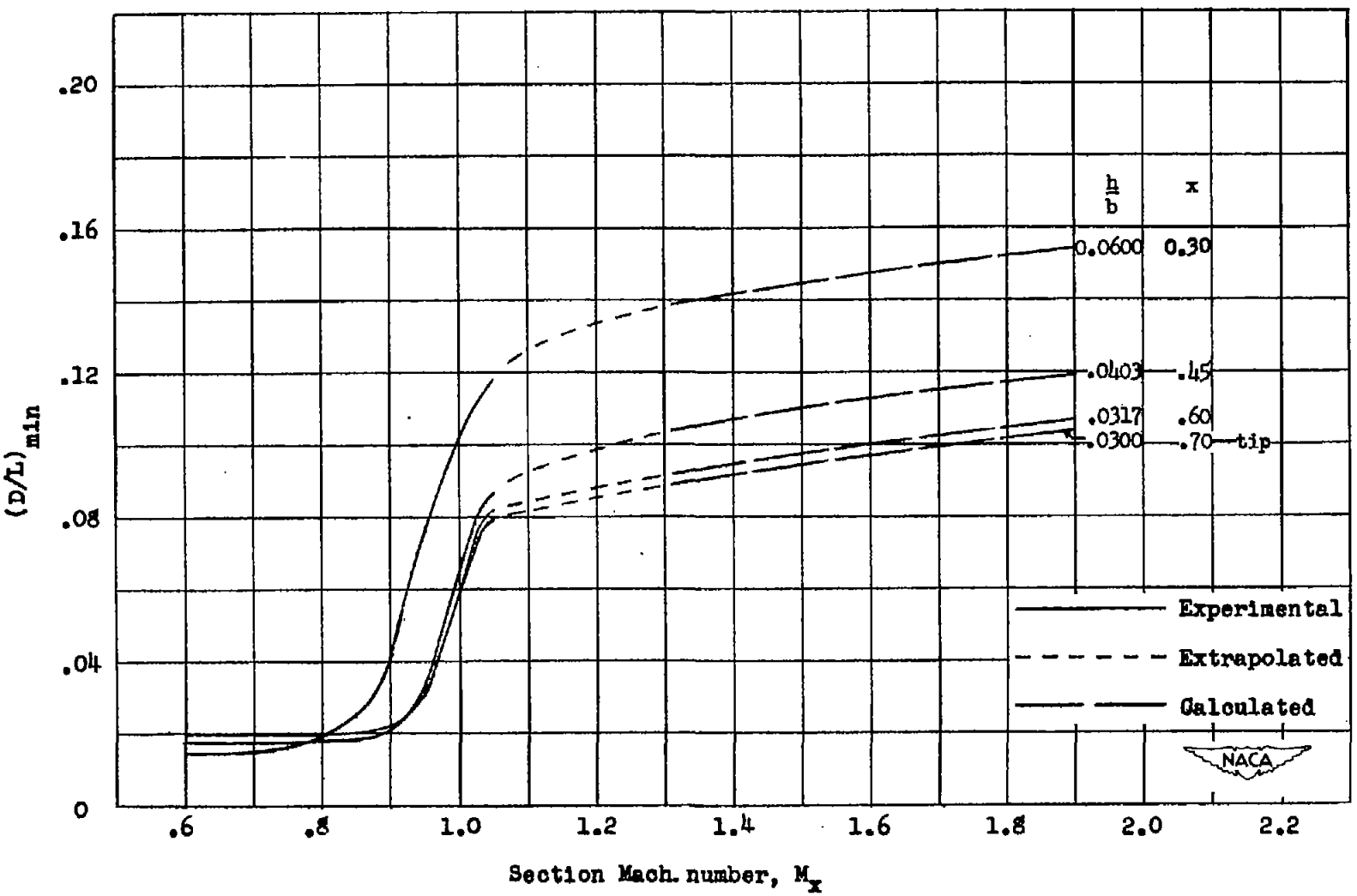

Figure 4.- Minimum drag-lift ratio against section Mach number for various thickness ratios with corresponding radial location for example thin propeller.

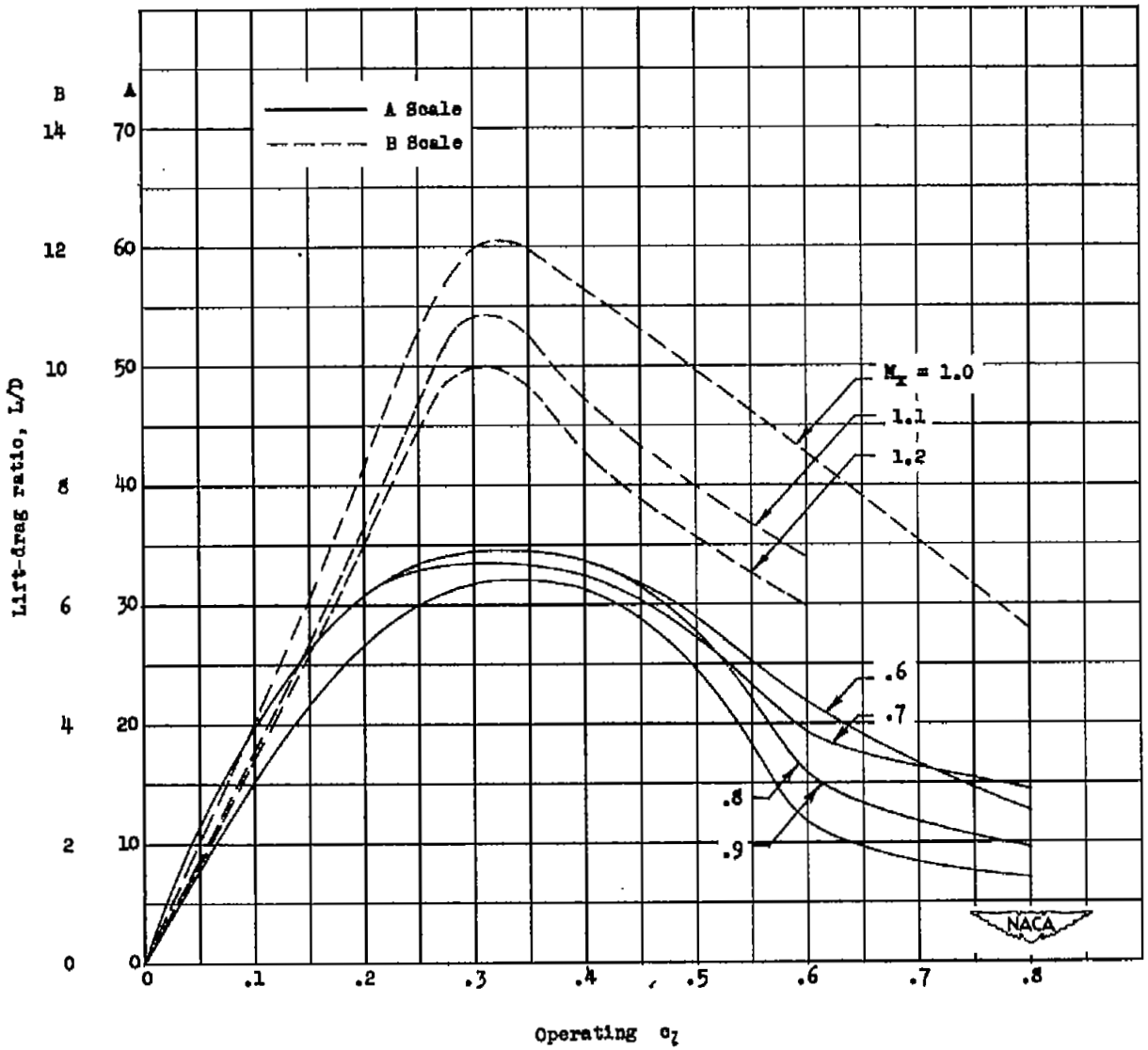

Figure 5.- L/D against operating c_l at constant section Mach number. NACA 16-004 airfoil.

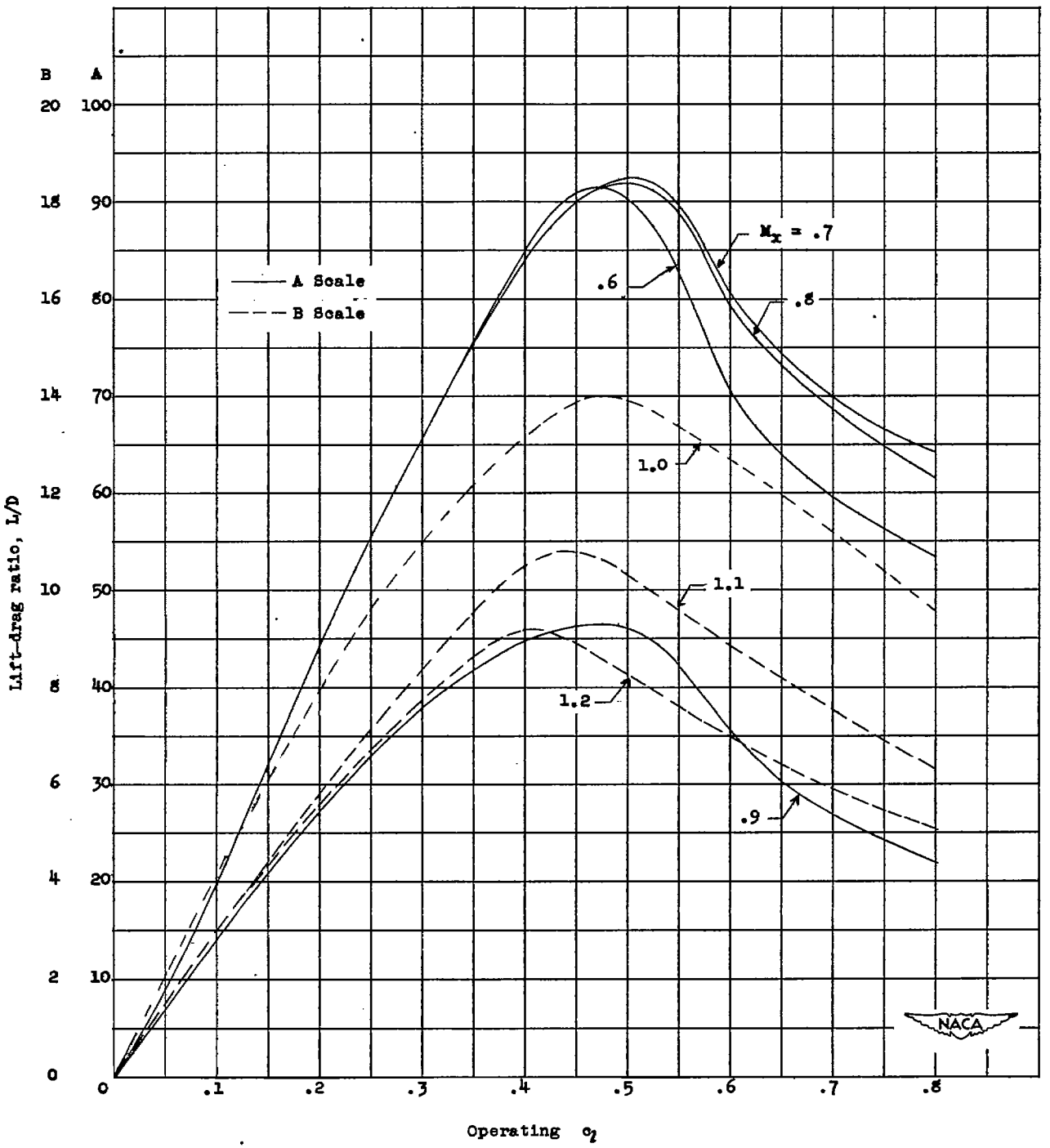

Figure 6.- L/D against operating c_l at constant section Mach number. NACA 16-304 airfoil.

[redacted]

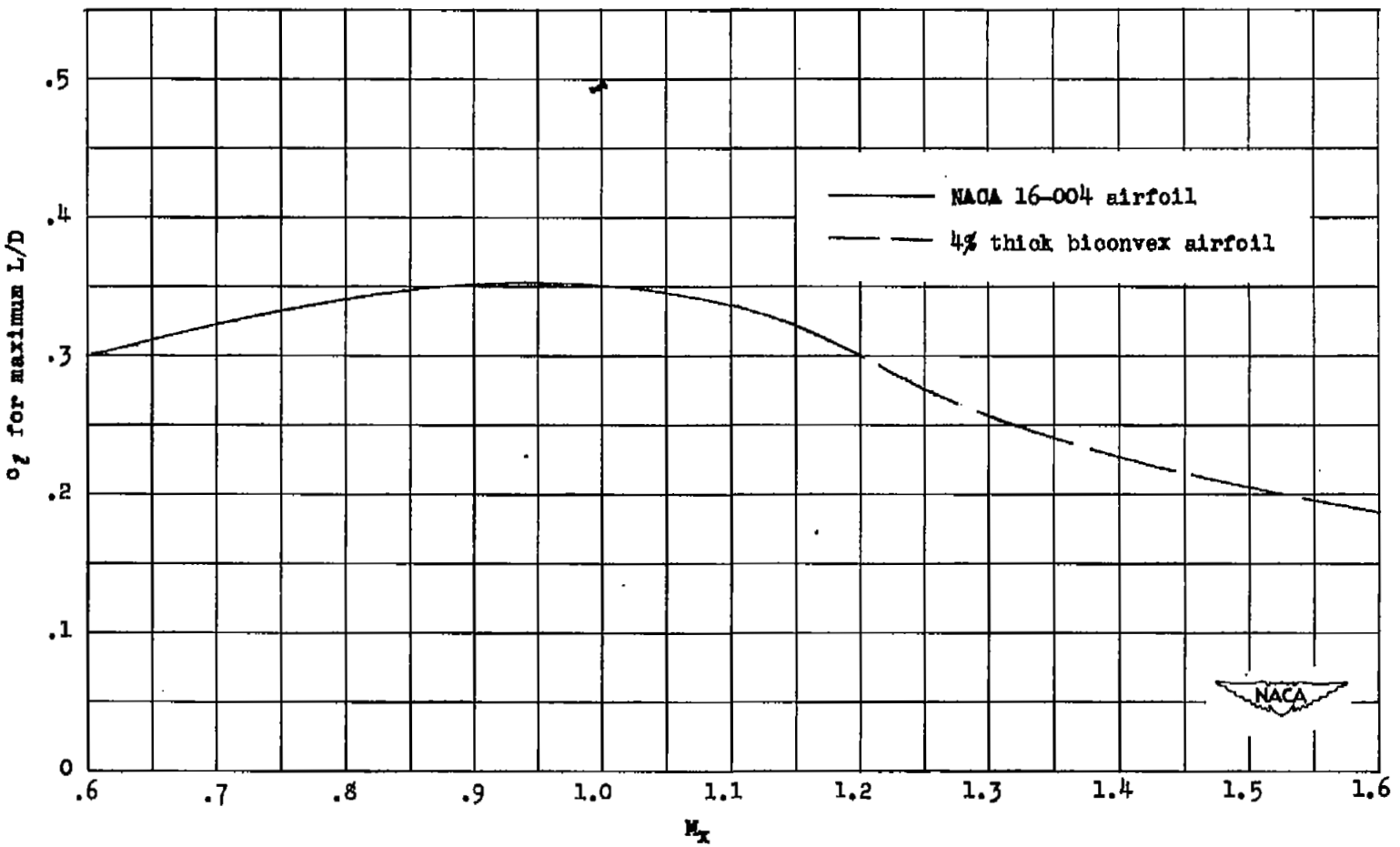

Figure 7.- Variation of c_l for maximum L/D. Symmetrical airfoil; $\frac{h}{b} = 0.04$.

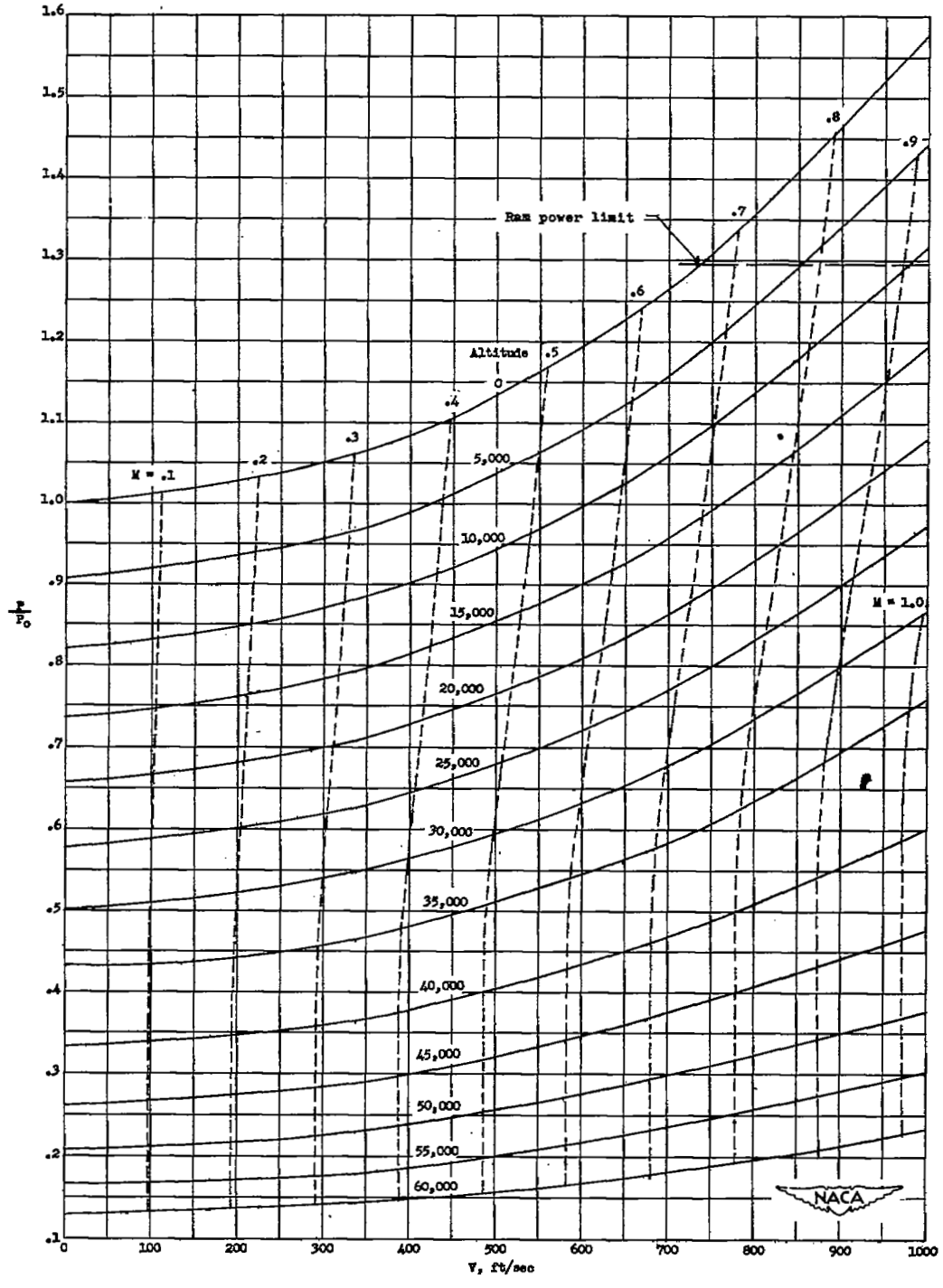

Figure 8.- Typical maximum shaft horsepower of turboengine in terms of the maximum shaft horsepower at V = 0 and NACA standard sea-level air.

[redacted]

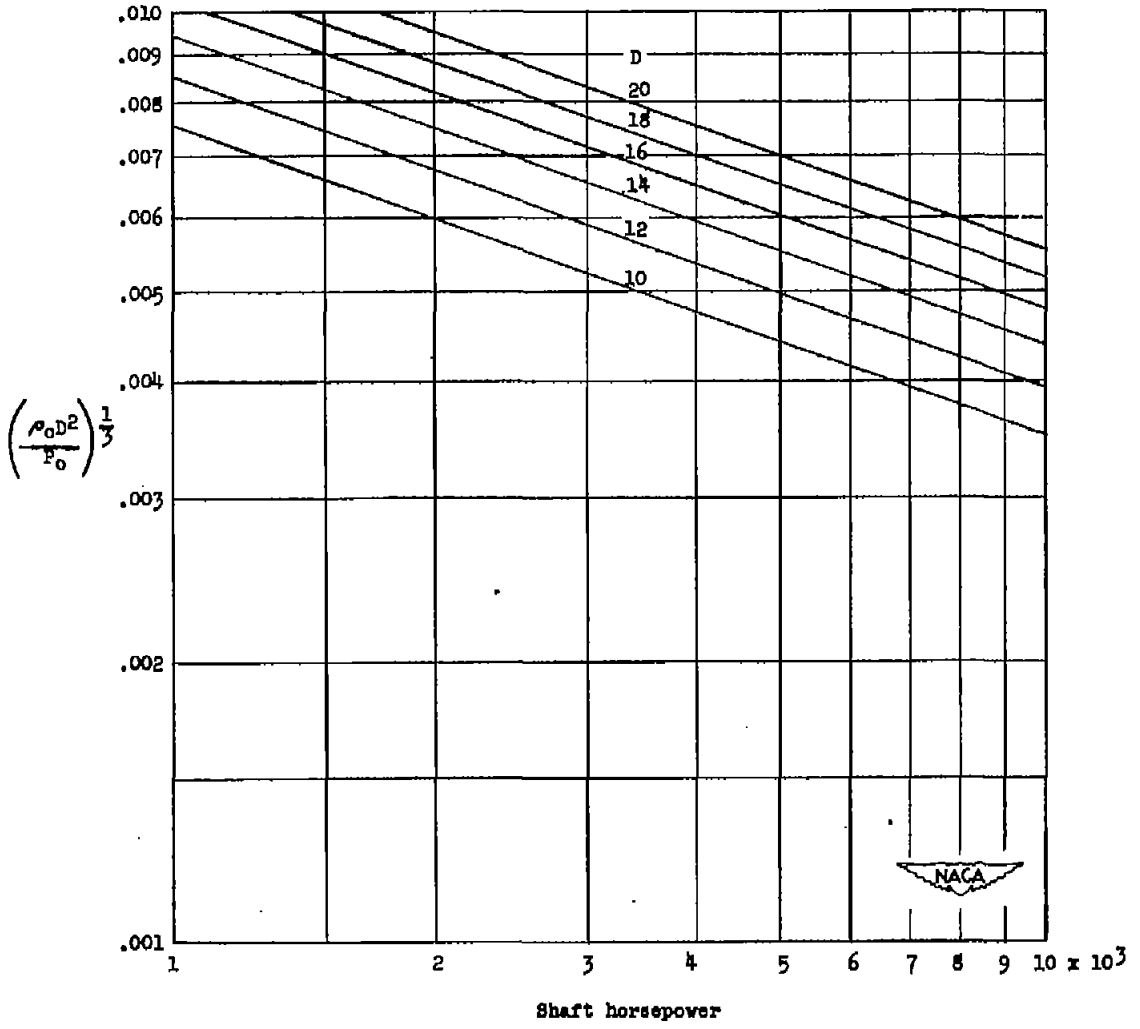

Figure 9.- Quantity $\left(\frac{\rho_o D^2}{P_o}\right)^{1/3}$ against shaft horsepower at constant diameter.

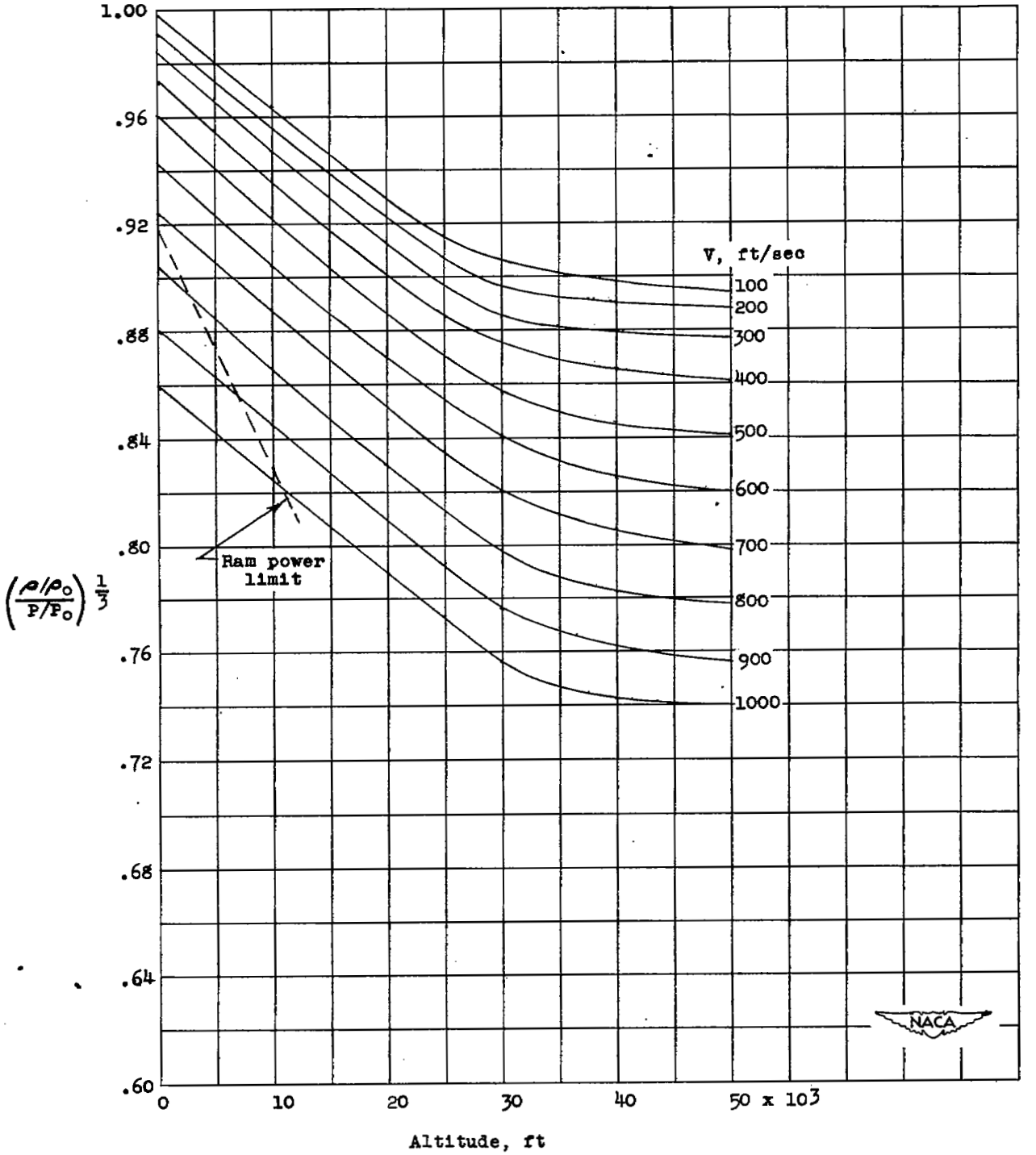

Figure 10.- Quantity $\left(\frac{\rho/\rho_0}{P/P_0}\right)^{1/3}$ as a function of velocity and altitude.

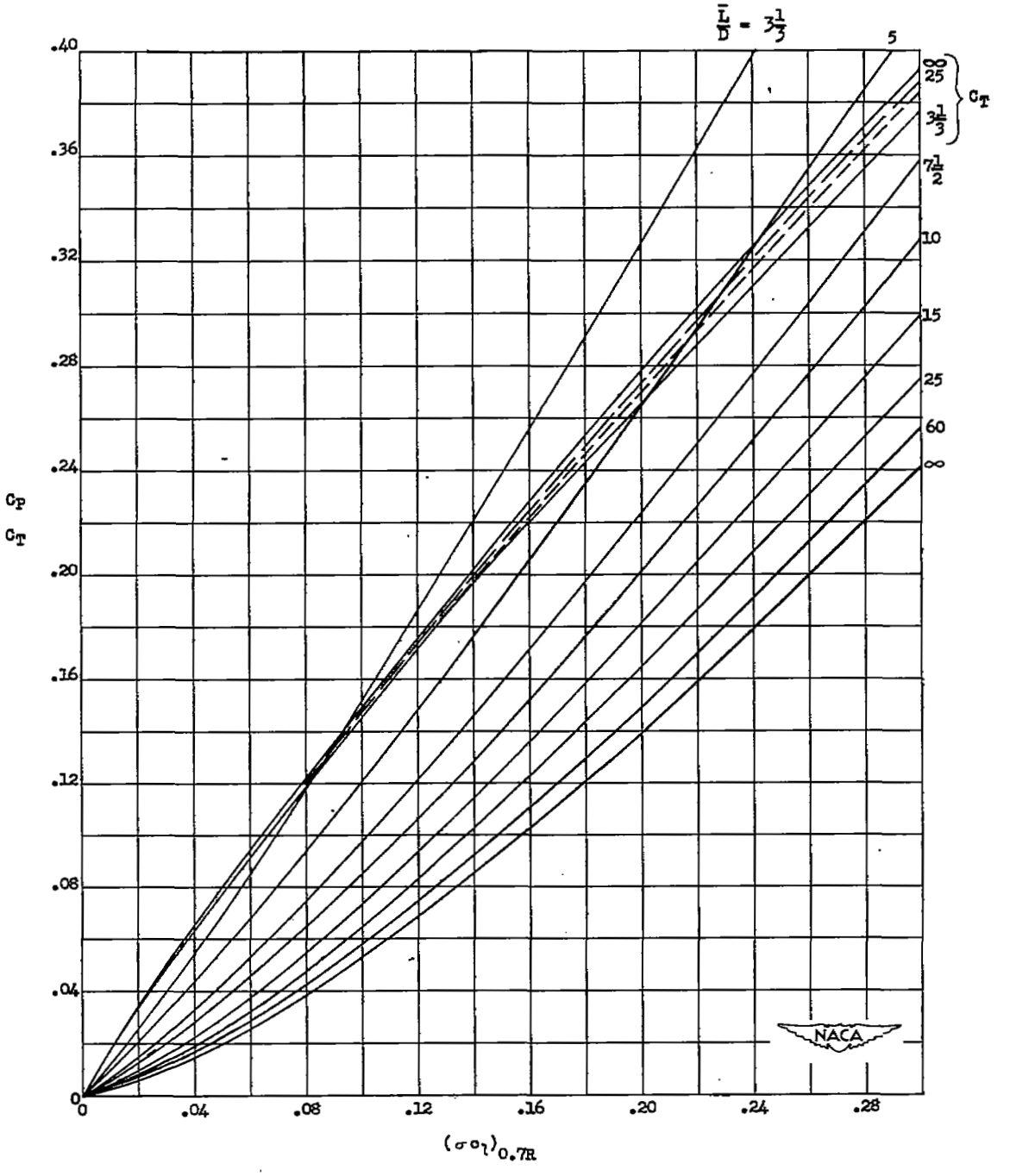

Figure 11.- C_P and C_T as functions of $(\sigma c_l)_{0.7R}$ for various values of constant L/D. Optimum load distribution.

[redacted]

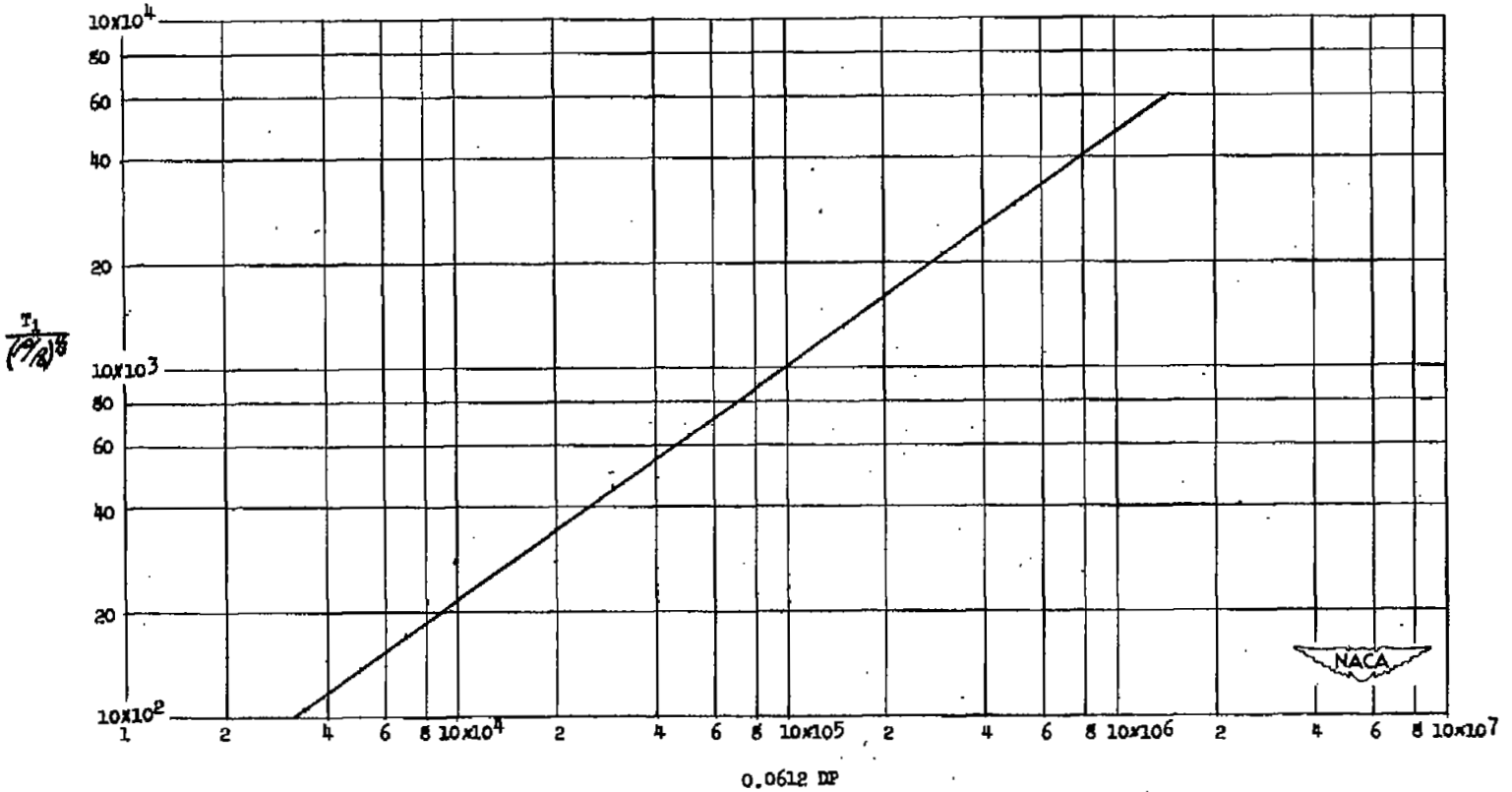

Figure 12.- Ideal static thrust as a function of the product of the diameter and the power.

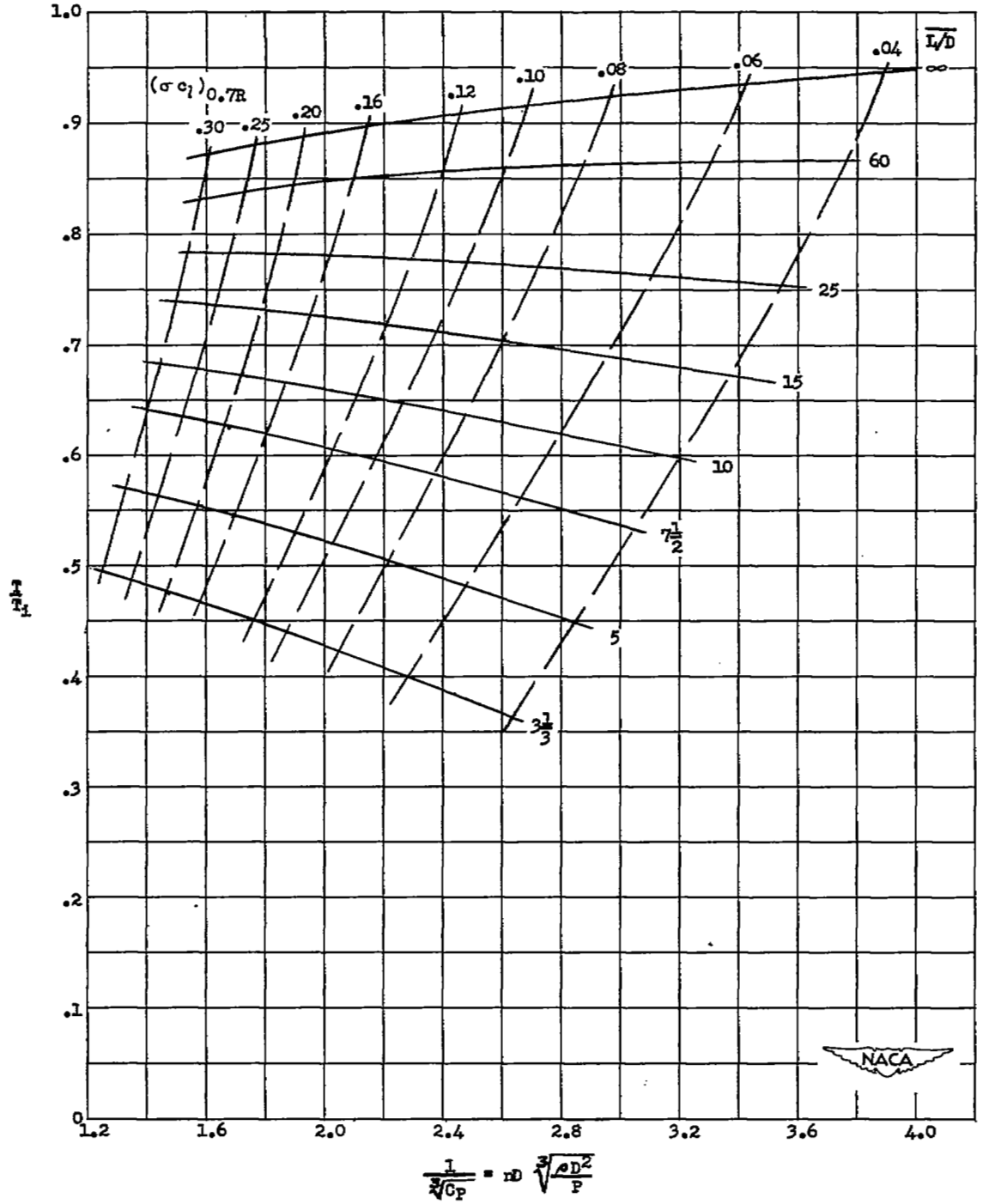

Figure 13.- Ratio T/T_1 as a function of $1/\sqrt[3]{C_P}$ for various values of $(\sigma c_l)_{0.7R}$ and $\overline{L/D}$. Four-blade propellers; J = 0.

[redacted]

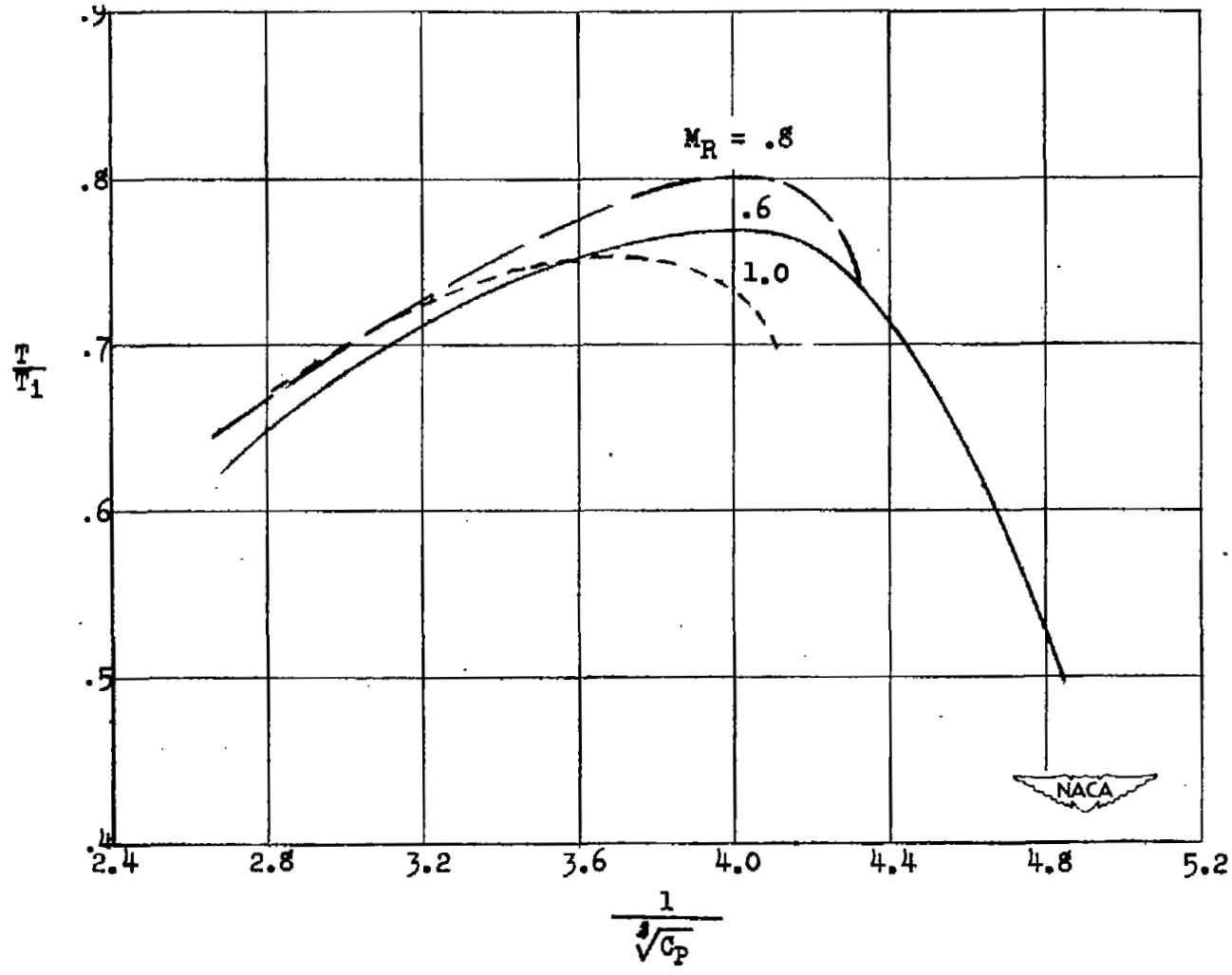

Figure 14.- Data for NACA 10-(5)(066)-03 two-blade propeller to show T/T_i as a function of rotational speed.

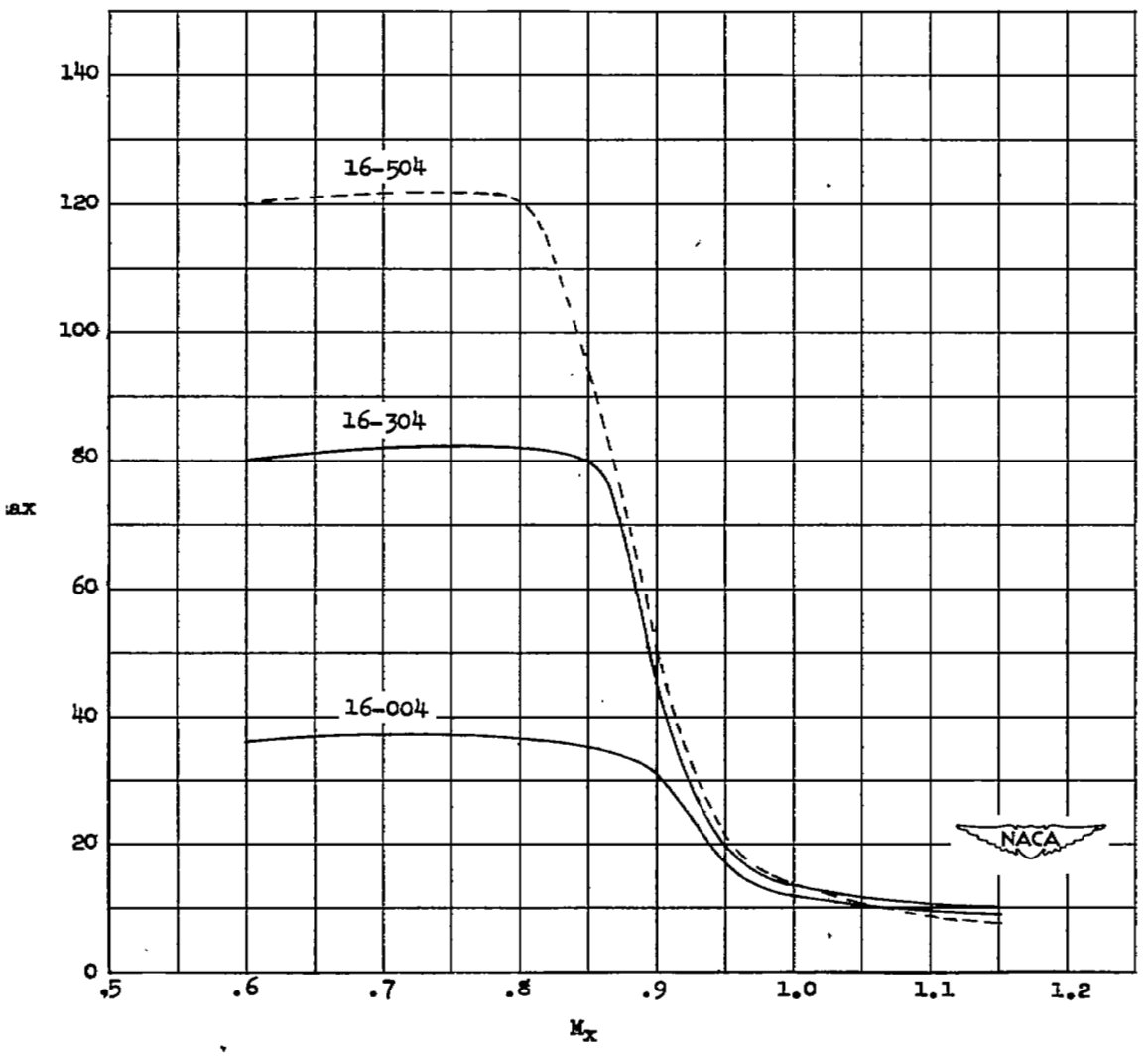

Figure 15.- Variation of maximum L/D with section Mach number. NACA 16-series airfoils.

[redacted]

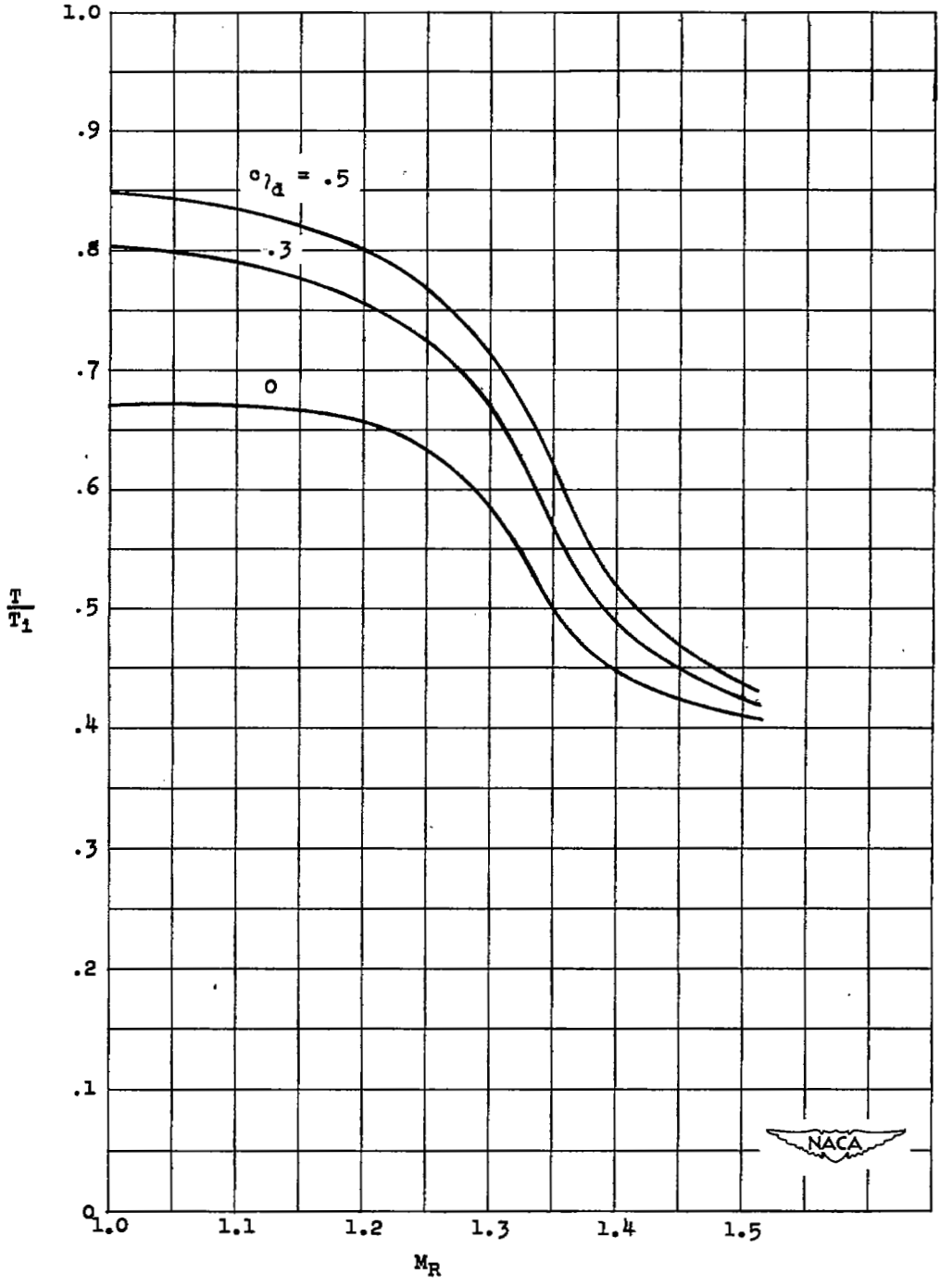

Figure 16.- Estimated peak T/T_1 as a function of rotational tip Mach number. Camber varying. $\left(\frac{h}{b}\right)_{0.7R} = 0.04$; B = 4; $\sigma_{0.7R} = 0.16$.

DO NOT REMOVE SLIP FROM MATERIAL

Delete your name from this slip when returning material to the library.

NAME	MS
R. Pegg	350

NASA Langley (Rev. May 1988) RIAD N-75